

New Multitarget Molecules Derived from Caffeine as Potentiators of the Cholinergic System

Juan Pablo Munafó, Brunella Biscussi, Diego Obiol, Marcelo Costabel, Cecilia Bouzat, Ana Paula Murray, and Silvia Antollini*



Cite This: <https://doi.org/10.1021/acschemneuro.3c00710>



Read Online

ACCESS |



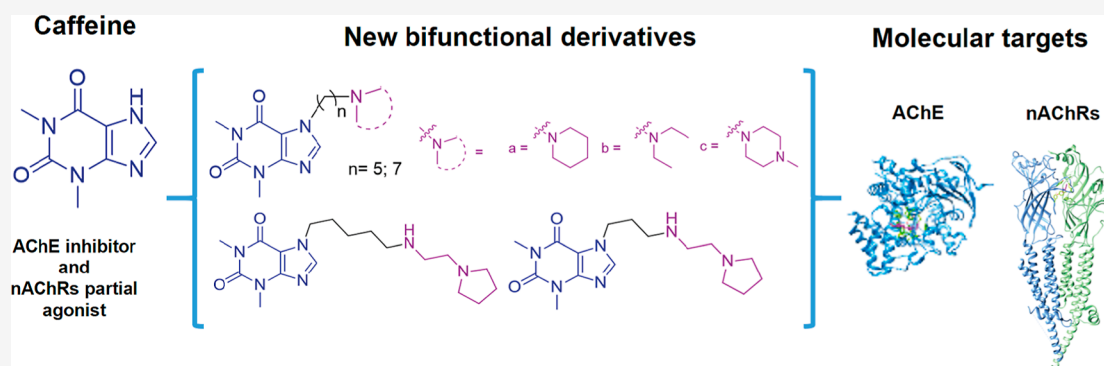
Metrics & More



Article Recommendations



Supporting Information



ABSTRACT: Cholinergic deficit is a characteristic factor of several pathologies, such as myasthenia gravis, some types of congenital myasthenic syndromes, and Alzheimer's Disease. Two molecular targets for its treatment are acetylcholinesterase (AChE) and nicotinic acetylcholine receptor (nAChR). In previous studies, we found that caffeine behaves as a partial nAChR agonist and confirmed that it inhibits AChE. Here, we present new bifunctional caffeine derivatives consisting of a theophylline ring connected to amino groups by different linkers. All of them were more potent AChE inhibitors than caffeine. Furthermore, although some of them also activated muscle nAChR as partial agonists, not all of them stabilized nAChR in its desensitized conformation. To understand the molecular mechanism underlying these results, we performed docking studies on AChE and nAChR. The nAChR agonist behavior of the compounds depends on their accessory group, whereas their ability to stabilize the receptor in a desensitized state depends on the interactions of the linker at the binding site. Our results show that the new compounds can inhibit AChE and activate nAChR with greater potency than caffeine and provide further information on the modulation mechanisms of pharmacological targets for the design of novel therapeutic interventions in cholinergic deficit.

KEYWORDS: nicotinic receptors, acetylcholinesterase, caffeine analogues, conformational state, electrophysiology, docking

INTRODUCTION

Acetylcholine (ACh), which is the main character of the cholinergic system, is a neurotransmitter widely distributed throughout the body with numerous essential physiological functions. The cholinergic system involves two types of acetylcholine receptors, namely, nicotinic (nAChR) and muscarinic receptors (mAChR). The differences between them lie not only in the body location/distribution but also in the signaling cascade that they initiate. Whereas nAChR is a ligand-gated ion channel causing the excitation of the postsynaptic membrane, mAChR is a metabotropic receptor triggering either excitation or inhibition of the postsynaptic membrane depending on its associated G-protein.

The nAChR is an integral membrane protein that belongs to the Cys-loop superfamily of ligand-gated ion channels.^{1,2} ACh binding causes sequential conformational changes that lead to the opening of a channel, the passage of positive ions across the

membrane, and the depolarization of the postsynaptic membrane.^{3,4} nAChR can be found in the central nervous system, in the peripheral neural system—the most characterized being those at the neuromuscular junction—and in peripheral non-neural cells (*i.e.*, epithelial and immune cells).⁵ They are pentameric proteins, and their identity depends on the subunit combination. In vertebrates, there are 17 different nAChR subunits ($\alpha 1$ – $\alpha 10$, $\beta 1$ – $\beta 4$, γ , δ , and ϵ) which can form heteromeric or homomeric receptors, each one having a specific structure, function, and location.^{6–9} In particular, embryonic

Received: November 1, 2023

Revised: January 3, 2024

Accepted: January 29, 2024



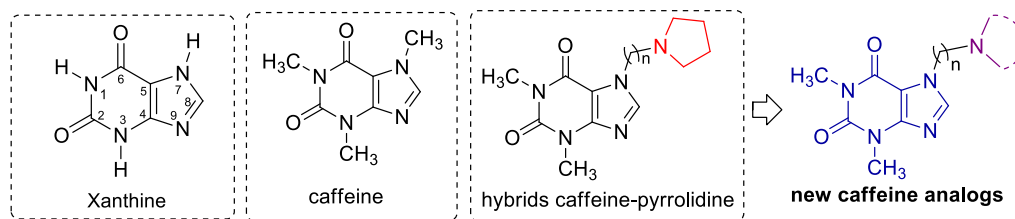


Figure 1. Xanthine core, chemical structures of caffeine and caffeine–pyrrolidine hybrids (AChE inhibitors and nAChR modulators), motifs for the design of new multitarget caffeine analogues.

muscle nAChR and muscle-type nAChR from *Torpedo californica* electric organ are formed by a $\alpha 1\beta 1\delta\gamma$, whereas adult muscle nAChR changes the γ subunit to the ϵ subunit. In the central nervous system, the two most relevant receptors are the heteropentamer $\alpha 4\beta 2$ and the homopentamer $\alpha 7$.^{10–13} The latter is particularly important for Alzheimer's disease (AD).¹⁴

Neurotransmitter and receptors are crucial but not enough for a proper cholinergic system. The enzyme acetylcholinesterase (AChE) is a necessary partner for the limitation of the ACh stimulus. AChE, a globular nontransmembrane protein, can be in multiple molecular forms depending on the cell type and cellular compartment.¹⁵ In the central nervous system, AChE is mainly found as G4, a tetrameric AChE_T (T peptide: C-terminal α -helix peptide of 40 amino acids) bound to PRiMA (proline-rich membrane anchor).¹⁶ Each AChE has two interesting sites: the active or catalytic site (CAS) and a more exposed peripheral anionic site (PAS), at approximately 20 Å from the CAS site. PAS has several noncholinergic functions, out of which its interaction with the amyloid β -peptide contributing to fibril aggregation^{17,18} is of great pharmacological interest.

The cholinergic system is involved in several physiological functions, such as muscle contraction. In the central nervous system, it is involved in growth, development, and aging-regulating neural plasticity, differentiation, proliferation, and clearance of aged neurons.¹⁹ It is also involved in a large variety of pathophysiological conditions, such as different myasthenic syndromes, myasthenia gravis, in particular, Alzheimer's disease (AD), the most prevalent neurodegenerative disorder in the elderly characterized by progressive cognitive decline, Tourette syndrome, and nocturnal frontal lobe epilepsies, among others.^{20–26} Although the occurrence of these different pathophysiological conditions is due to different causes—multifactorial events in some cases—from a therapeutic point of view, they can be classified into two main groups. One group includes the first two above-mentioned pathological conditions, among others, sharing the “cholinergic hypothesis” that is related to a deficit of functional nAChR, and hence nAChR function potentiation is the therapeutic goal (muscle nAChR in the case of myasthenic syndromes and neuronal nAChR for AD, becoming $\alpha 7$ nAChR increasingly more important for AD pathology²⁷). In the case of the second group, which is exactly the opposite to the first group and which includes the two last above-mentioned conditions, there is a gain of nAChR function, and hence, the seeking of an antagonistic or desensitized effect is the pharmacological goal. As stated above, although there are different nAChR having distinct pharmacological profiles, muscle and $\alpha 7$ nAChR, both involved in myasthenic syndromes and in AD, are inhibited by α -bungarotoxin (α -BTX).²⁸ Great efforts are made to find new treatments for these diseases, and although the potentiation of the cholinergic system will not solve these pathological conditions, until now it is the main pharmacological strategy.²⁹

Through previous research, we identified caffeine as a new leader that can inhibit AChE and activate both muscle and $\alpha 7$ nAChR.³⁰ Caffeine behaves as a partial agonist at low micromolar concentrations and as an ion channel blocker at high micromolar concentrations. We then synthesized several caffeine derivatives connecting theophylline with pyrrolidine with a linker of a different number of carbon atoms. All of the resulting compounds were AChE inhibitors. Interestingly, the derivatives with a linker between 5 and 7 carbon atoms showed the highest nAChR potentiation. Furthermore, whereas analogues with a linker of 5 C atoms showed nAChR activation and also receptor desensitization, those analogues with a linker of 7 C atoms did not cause nAChR desensitization.³¹ Recently, compounds derived from caffeine, achieved through chemical modifications of theophylline, theobromine, or acefylline, have also been identified as inhibitors of the acetylcholinesterase enzyme.^{32–35} This strategy, involving the combination of diverse pharmacophores or functional groups derived from theophylline and its derivatives, has proven effective in enhancing the activity of the original pharmacological compounds, as demonstrated in our previously synthesized series of caffeine derivatives.³¹ However, these reports evaluated only the effect on AChE and not on nAChR. Furthermore, almost all of these compounds exhibited lower AChE inhibitory potency than our previous caffeine analogues. Only in the work of Reshetnikov *et al.* did a few derivatives achieve nanomolar AChE inhibitory potencies.³²

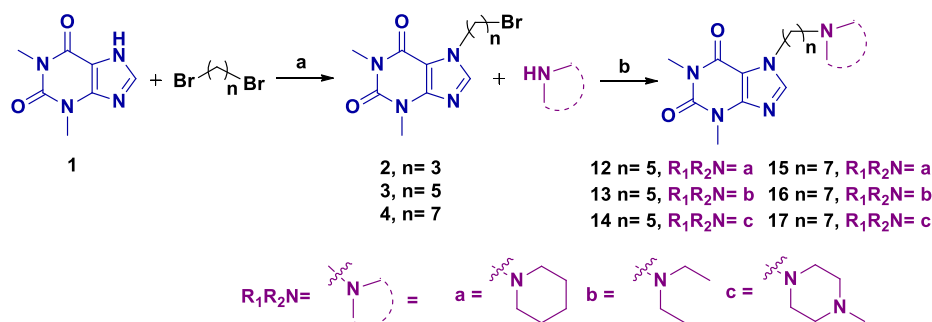
As a follow-up to prior research, this study undertakes the synthesis of novel caffeine derivatives using theophylline as the starting material and various secondary amines. Additionally, derivatives were prepared that incorporate an NH functional group in the hydrocarbon chain of the linker with the aim of achieving enhanced interactions with both the enzyme and the receptor (Figure 1). This strategy enabled us to obtain a series of new caffeine analogues that, unlike previously reported derivatives, displayed intriguing and potent dual activity against acetylcholinesterase (AChE) and nicotinic receptors (nAChR), with IC₅₀ values in the nanomolar range.

RESULTS AND DISCUSSION

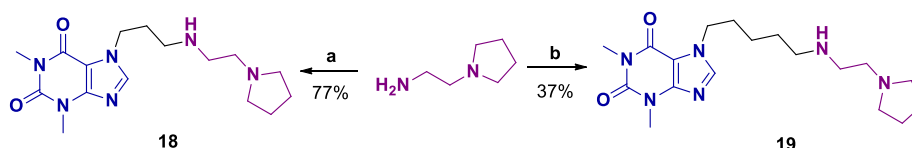
In the present work, we focused on the design and synthesis of novel caffeine derivatives with dual activity on both AChE and nAChR, which exhibit greater potency than our previously reported caffeine–pyrrolidine hybrids.³¹ To this end, we introduced a variety of amino residues linked through a variable length hydrocarbon chain (with or without an NH functional group) to the N-7 position of theophylline. Our approach was based on our experience and understanding of the impact of this synthesis strategy on the pharmacological activity of this kind of derivatives.

We chose to synthesize derivatives with a 5 and 7 carbon linker based on results from a previous study from our lab.³¹ In

Scheme 1. Synthesis of Derivatives 2–4 and 12–17: (a) Anh K₂CO₃, Dry dimethylformamide (DMF), and MW (10 min, 80 °C) and (b) Dry DMF and MW (5–10 min, 150 W)



Scheme 2. Synthesis of Derivatives 18 and 19^a



^aReagents and conditions: (a): 7-(3-bromopropyl)-1,3-dimethyl-3,7-dihydro-1H-purine-2,6-dione, dry DMF, RT (4 h). (b): 7-(5-bromopentyl)-1,3-dimethyl-3,7-dihydro-1H-purine-2,6-dione, dry DMF, RT (4 h).

Table 1. AChE Inhibitory Capacity of Caffeine Derivatives Expressed in IC₅₀ Values

compound	linker	amino group	IC ₅₀ (μM) (95% CI)
caffeine ^a			87.01 ^a (75.01–100.93)
theophylline ^b			473.02 ^b (321.5–696.0)
7 ^b	–(CH ₂) ₃ –	pyrrolidine	56.24 ^b (48.29–65.45)
8 ^b	–(CH ₂) ₄ –	pyrrolidine	21.75 ^b (17.50–27.02)
9 ^b	–(CH ₂) ₅ –	pyrrolidine	13.52 ^b (11.89–15.33)
10 ^b	–(CH ₂) ₆ –	pyrrolidine	6 × 10 ² (4.92–7.55)
11 ^b	–(CH ₂) ₇ –	pyrrolidine	0.220 ^b (0.161–0.289)
12	–(CH ₂) ₅ –	piperidine	1.42 (1.24–1.62)
13	–(CH ₂) ₅ –	diethylamine	6.01 (5.28–6.85)
14	–(CH ₂) ₅ –	1-methylpiperazine	4.29 (3.74–492)
15	–(CH ₂) ₇ –	piperidine	0.601 (0.397–0.908)
16	–(CH ₂) ₇ –	diethylamine	0.326 (0.287–0.371)
17	–(CH ₂) ₇ –	1-methylpiperazine	2.75 (2.08–3.63)
18	–(CH ₂) ₃ –NH–(CH ₂) ₂ –	pyrrolidine	1.81 (1.44–2.27)
19	–(CH ₂) ₅ –NH–(CH ₂) ₂ –	pyrrolidine	0.046 (0.042–0.050)
tacrine			0.029 (0.022–0.040)

^aRef 30. ^bRef 31.

this previous study, we reported that the caffeine–pyrrolidine hybrid with a linker of seven carbon atoms displayed the highest potency in inhibiting AChE and activating nAChRs in the picomolar range. Interestingly, this hybrid did not induce receptor desensitization. On the other hand, the hybrid with a five-methylene group also inhibited AChE and activated the receptor, but it led to a desensitized state of the receptor.

Synthesis of Caffeine Derivatives. The novel compounds 12–17 were synthesized according to Scheme 1. The first step to obtain alkylbrominated intermediates of theophylline was carried out as previously reported.³¹ The reaction with the corresponding secondary amine was subsequently performed to

obtain the desired products. Each of the synthetic steps was carried out in a microwave reactor (CEM Discover) in less than 10 min.

Next, we focused our efforts on the design and synthesis of novel caffeine–pyrrolidine hybrids containing an NH functional group in the hydrocarbon chain (synthetic compounds 18 and 19) to increase the potential of hydrogen-bond interactions with both the enzyme and the receptor and, thus, improve biological activity. To this end, the same synthesis strategy as that followed for compounds 12–17 was used, although with some modifications, using the bromoalkylated intermediate of

Table 2. Binding Energy and Interacting Residues from AChE Docking Studies^a

	Interacting residues									
	Donepezil	Tacrine	Comp 12	Comp 13	Comp 14	Comp 15	Comp 16	Comp 17	Comp 18	Comp 19
Benzyl group (donepezil) / tacrine / Theophylline group (comp 12-19)	W86	W86 G121 Y124	D74 W86 G121	D74 W86 G121	D74 W86 G121	D74 W86 G121	D74 W86 G121	D74 W86 G121	W86 G121 G122 Y124	Y72 Y124 W286 F295 Y337 F338 Y341
	E202 S203	E202 S203			F295				S203	
		F297 Y337 F338 Y341								
	H447	H447				H447	H447	H447	H447	
Piperidine group (donepezil) / Linker (comp 12-19)	D74									W86
	Y124		Y124						G122	
	Y337		Y337	Y337	Y337	F297 Y337 F338 Y341	F297 Y337 F338	F297 Y337 F338		Y337
	Y341		H447	Y341 H447	H447	H447	H447	H447		Y341
Dimethoxyindanone (donepezil) / "other group" (comp 12-19)	Y72								D74	G121 G122
			Y124	Y124	Y124	Y124	Y124	Y124		S203
	W286		W286	W286	W286	W286	W286	W286		
	F295		F295	F297 F338 Y341	F295	F338 Y341	F338 Y341	F338 Y341		F297 F338
BBE (Kcal/mol)	-12.3	-12.1	-9.4	-8.4	-9.1	-9.8	-8.6	-9.5	-8.7	-8.7

^aThe best binding energy (BBE) of the most stable conformation obtained after docking analyses is shown for each ligand. All the interacting residues observed in the different conformations are listed for each ligand. The residues reported as relevant for enzymatic activity are shown in bold (with residues from the CAS site in black and from the PAS site in gray). Data correspond to 10 independent docking experiments.

theophylline and 2-pyrrolidin-1-yl-ethanolamine as starting materials (Scheme 2).

The reaction with 2-(pyrrolidin-1-yl)ethanamine posed some challenges as the reaction mixture yielded undesired side products. This required an extensive purification process to obtain the desired product. Due to the highly polar nature of the product, it was necessary to use a chromatographic column with a mobile phase consisting of a mixture of dichloromethane and methanol, to which 1% triethylamine was added. This allowed us not only to achieve a high level of purification but also to obtain the desired product. As can be seen in Scheme 2, microwave heating was avoided and the reaction was carried out at room temperature for 4 h.

AChE Enzyme Inhibition. All new compounds were evaluated for their ability to inhibit AChE by Ellman's spectrophotometric method. In previous research from our lab, we observed that both caffeine³⁰ and a series of its derivatives (compounds 7–11)³¹ inhibited AChE (Table 1).

In the present work, we found that compounds having a linker of seven carbon atoms showed higher inhibitory activity than the ones having a linker of five carbon atoms, similar to what we observed previously with other derivatives (compounds 9 and 11). Compounds 12–14, with a linker of five carbon atoms,

were found to be more effective inhibitors compared to compound 9 (previously, a caffeine derivative with five carbon atoms). In contrast, the new derivatives with a 7-methylene linker exhibited lower inhibitory activity than compound 11, also with a linker of seven carbon atoms, and showed in compound 16 the closest inhibitory potency value to that of compound 11. However, introducing an NH substituent into the 7-methylene linker showed highly favorable results. In fact, compound 19, with this NH substitution, turned out to be the most potent inhibitor in the series, displaying an IC₅₀ in the nanomolar range (IC₅₀ = 46 nM), similar to tacrine (IC₅₀ = 29 nM).

Taking into account that some AChE inhibitors may also inhibit butyrylcholinesterase (BChE), we decided to conduct a preliminary assay of BChE inhibition at a concentration of 20 M, and it was observed that none of the theophylline derivatives obtained in this work were able to inhibit BChE at that concentration (data not shown). Consequently, these compounds can be considered selective AChE inhibitors.

In Silico Binding of Synthetic Caffeine Analogues to AChE. To test the interactions that each compound could have with AChE, molecular docking studies were performed. We used the structure 4EY7.pdb crystallized in complex with the

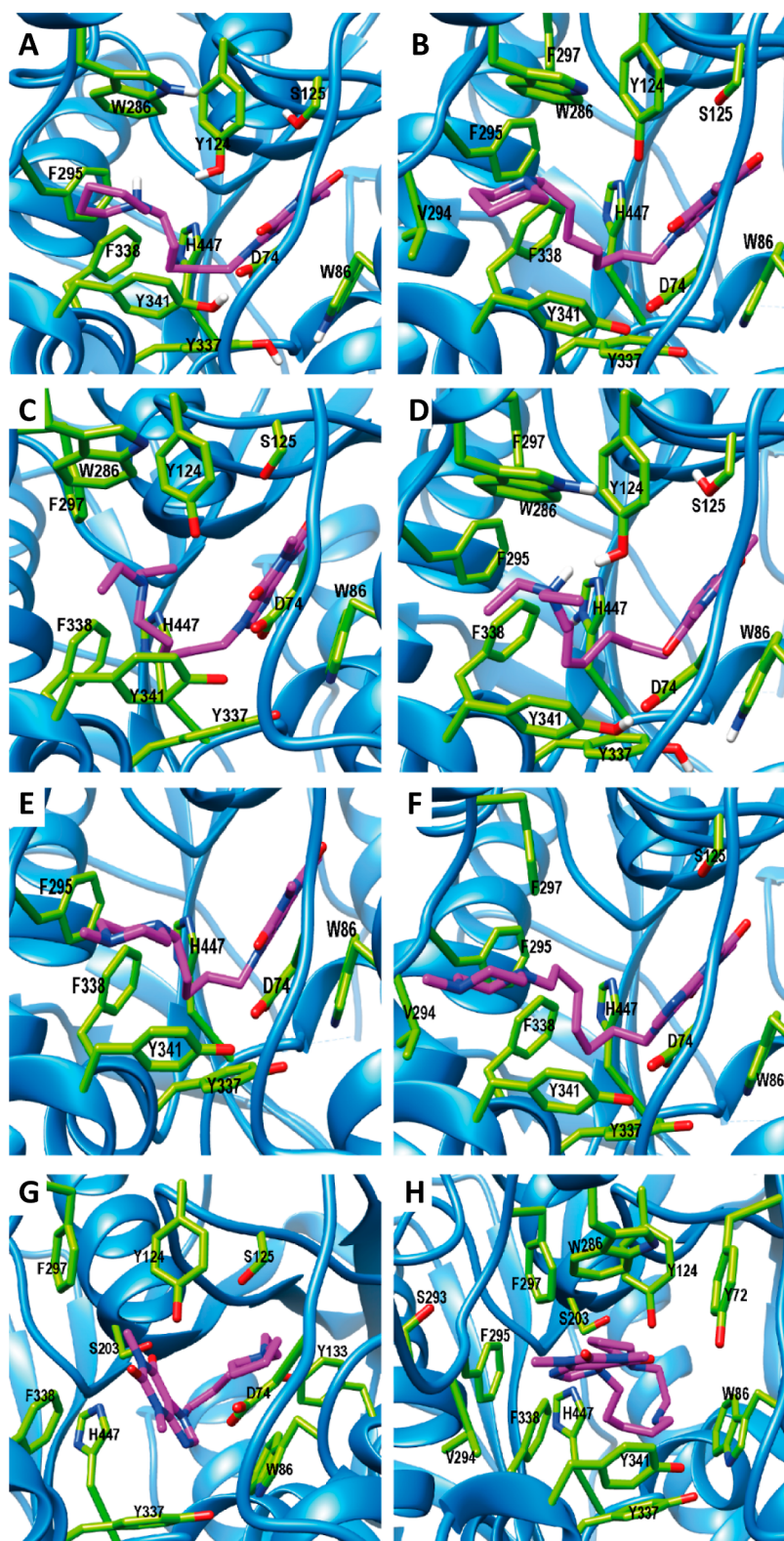


Figure 2. Molecular docking into the CAS/PAS site of the human AChE (4EY7.pdb). Detailed 3D structure of AChE showing the best conformation bound for caffeine derivatives: (A) **compound 12**, (B) **compound 13**, (C) **compound 14**, (D) **compound 15**, (E) **compound 16**, (F) **compound 17**, (G) **compound 18**, and (H) **compound 19**. Compounds are shown as violet sticks, the surrounding residues in the binding pockets are shown as green sticks, and the backbone of the enzyme is shown in light blue.

donepezil molecule.³⁶ The AChE structure shows donepezil bound to the active site with the dimethoxyindanone ring located at the PAS site and the benzyl group located at the CAS site.¹⁸ Therefore, for these molecular docking studies, we

restricted the grid dimensions to the space that involves both the PAS and CAS sites. As an internal control, we first performed docking studies with donepezil (Figure S1A,B). The piperidine group showed cation– π interactions with residues D74 and

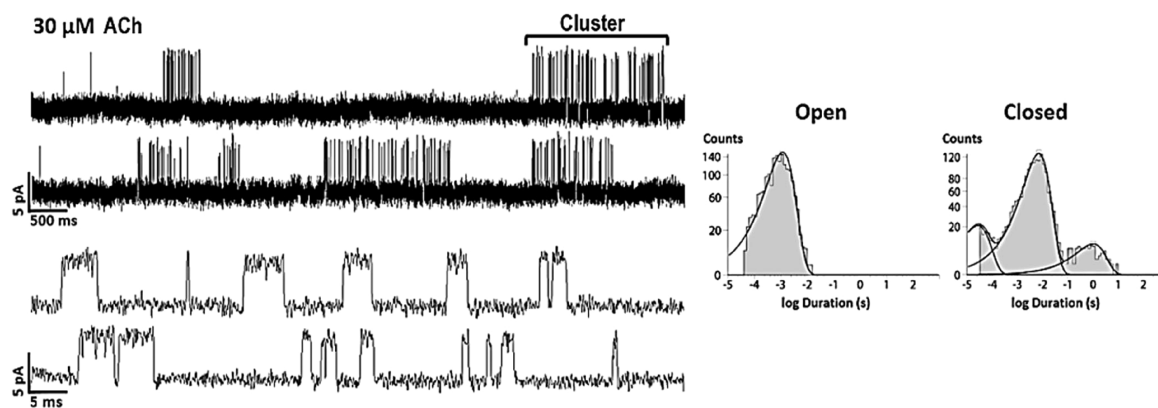


Figure 3. Representative single-channel events elicited by 30 μ M ACh recorded at -70 mV of membrane potential. Traces are shown at two different temporal scales. Openings are shown as upward deflections. Representative open- and closed-duration histograms are shown on the right.

Y337 and hydrophobic interactions with Y124, Y337, and Y341. The benzyl group formed π - π stacking interactions with residues W86 and H447 and hydrophobic interactions with W86, E202, H447, and S203. Additionally, the dimethoxyindanone group interacted by π - π stacking with residues W286 and Y341 and established H-bridge with F295 and hydrophobic interactions with Y72, Y341, and W286. All these interactions (Table 2) are similar to those that have already been reported in the crystalline structure.³⁶

As the tacrine molecule was used as an inhibition control in the experiments carried out to evaluate AChE activity, we additionally performed the docking of this molecule to observe its interactions with AChE (Figure S1C). The main conformation showed a score of approximately -12.0 kcal/mol, similar to donepezil. The tacrine molecule formed π -stacking interactions with Y337, Y341, and H447 and hydrophobic interactions with W86, G121, Y124, E202, S203, F297, Y337, F338, Y341, and H447. The amino group formed a H-bridge with G121. It is worthy of note that almost all interactions coincided with those observed with the benzyl group of donepezil (Table 2). Interestingly, most of these interactions have been reported as critical for AChE inhibition.^{36,37}

Caffeine analogues were subsequently docked on AChE using 10 independent assays. All of the analogues, except for **compound 18**, were located in the CAS/PAS sites (Figure 2). The binding scores were found in the ranges of -8.7 and -9.7 kcal/mol in all cases (Table 2). It was observed that, for the C5 and C7 linker analogues, the theophylline group was oriented toward the CAS site, whereas the piperidine, diethylamine, and methylpiperazine groups were oriented toward the PAS site. However, for **compound 19**, the pyrrole group was oriented toward the CAS site and the theophylline group toward the PAS site. The theophylline and pyrrole groups of **compound 18**, in particular, were located mostly in the CAS site (Figure 2G). The fact that it presented a potency similar to that of the other synthesized compounds clearly shows the crucial role that this site plays in AChE inhibition.

The molecular interactions of the different derivatives with linkers C5 and C7 were analyzed. It was found that the theophylline group of these derivatives, except for **compound 14**, formed π -stacking interactions with W86 and H-bridge with D74. Likewise, all of the derivatives tested showed hydrophobic interactions with W86 and G121. In contrast, the theophylline group of **compound 14** analogue formed a salt bridge with D74 and an H-bridge with F295 (Figure 2C).

In the case of the piperidine, diethylamine, and methylpiperazine groups of the derivatives with the C5 linker, it was observed that they formed an H-bridge with Y124 and hydrophobic interactions with W286, F338, Y341, and H447 (Figure 2A–C). In addition, while the piperidine and methylpiperazine groups formed hydrophobic interactions with F295, the diethylamine group formed this type of interaction with F297. Thus, the better potency of these compounds compared to that of the previously studied C5 analogue with pyrrole probably depends on a better interaction in the same sites because of the variation of the accessory group.

On the other hand, the derivatives with the C7 linker, in addition to the interactions observed for the analogues with the C5 linker, also established hydrophobic interactions with V294 (Figure 2D,E).

It was also observed as expected that at the level of the intermediate chain, the analogues with the C7 linker showed a higher number of hydrophobic interactions compared to the analogues with the C5 linker. While all C5 linkers formed hydrophobic interactions with Y337, the linker of **compound 13** also formed hydrophobic interactions with Y341 and the C5-piperidine derivative formed hydrophobic interactions with Y124. On the other hand, all C7 linkers formed hydrophobic interactions with F297, Y337, and F338. Apart from these interactions, the linker of **compound 15** also established these interactions with Y341 (Figure 2D).

As stated above, **compound 18** was located mainly in the CAS site of the enzyme, exhibiting π -stacking with W86, H-bridging with W86, Y124, Y133, G122, and S230, and hydrophobic interactions with D74 and W86 (Figure 2D).

Compound 19 localized in the two PAS/CAS sites with its pyrrole group oriented toward the CAS site and the theophylline group oriented toward the PAS site, contrarily to the analogues with C5 and C7 linkers. Both the pyrrole group and the linker formed hydrophobic interactions: the former with residues G121, G122, S203, F297, and F338 and the latter with residues W86, Y337, and Y341. The theophylline group established cation- π interactions with Y341, H-bridge with Y124 and F295, and hydrophobic interactions with W286, F338, and Y341 (Figure 2H). This analogue showed an inhibition potency of the same order of magnitude as tacrine. Its inverted location together with a cation- π interaction with Y341, an increment in length of the linker, and the presence of an amino group in the linker could probably explain the increase observed in the inhibition of AChE. Although all the compounds tested

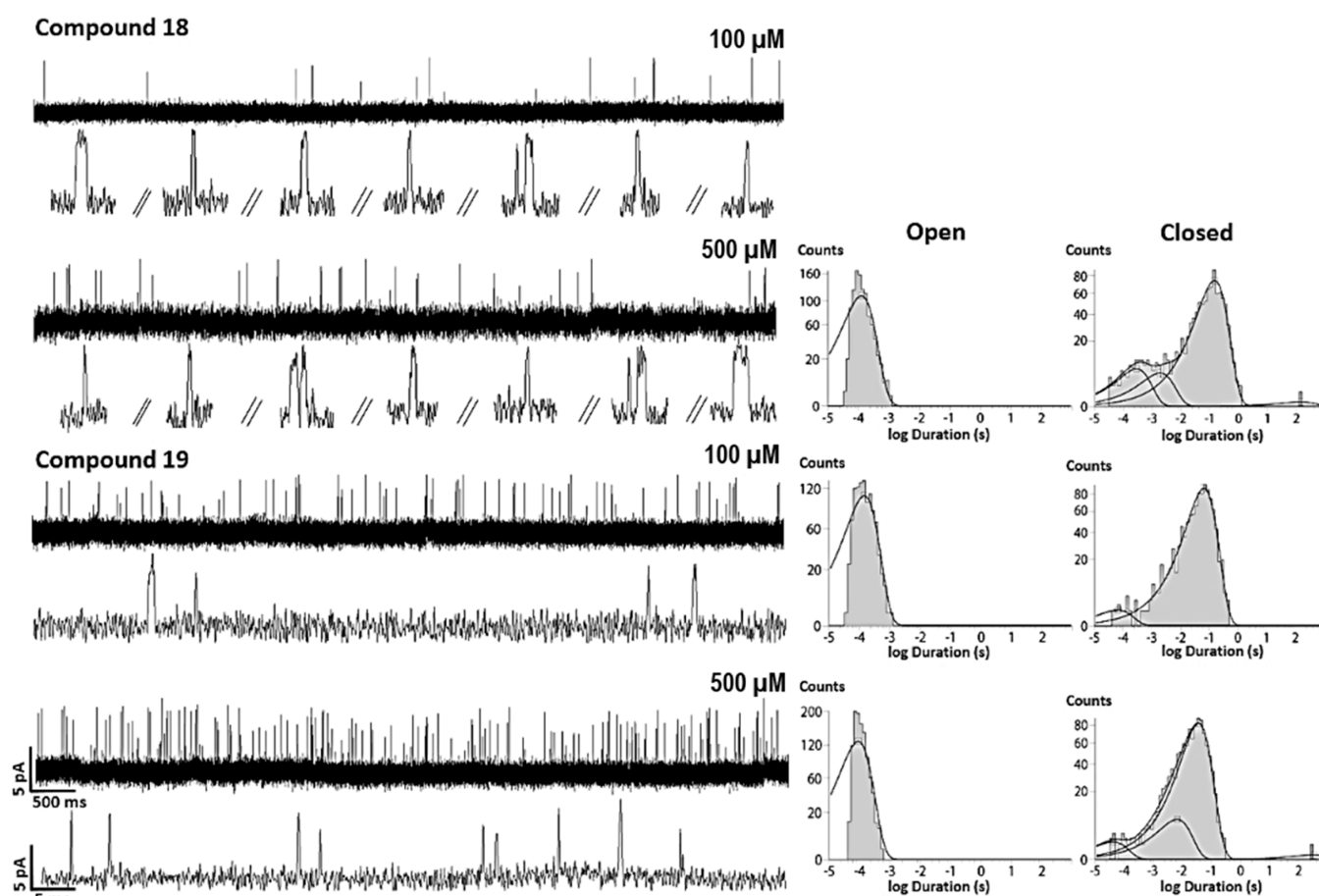


Figure 4. Muscle nAChR activation profile of compounds 18 and 19 at 100 and 500 μM , recorded at -70 mV of membrane potential. Openings are shown as upward deflections. Representative open- and closed-duration histograms for each condition are shown on the right.

interacted with Y341, only donepezil and tacrine formed interactions in the form of cation– π and π -stacking, respectively, similar to compound 19. It was also observed that certain inhibitors showed lower affinity for enzymes with the mutated Y341 amino acid.³⁸ All the compounds studied therefore inhibited AChE and made contacts with AChE residues which had been reported as relevant to inhibitor interactions.^{39–41} However, for a proper AChE inhibition to occur, to occupy only the CAS site (as it was observed with compound 18) or both the CAS and PAS sites is not enough, also it is necessary to form relevant interactions with Y341 of the PAS site (like compound 19).

nAChR Activation by Synthetic Caffeine Analogues.

We further studied if these caffeine derivatives maintain the AChR agonist activity previously reported for caffeine.³⁰ To this end, muscle nAChR was expressed in BOSC-23 cells, and single-channel currents elicited by ACh or by the different compounds were recorded.

Muscle nAChRs activated by ACh showed openings that are grouped into well-defined activation episodes called clusters.^{42,43} Each activation episode begins with the transition of a single receptor from the desensitized state to the activable state and terminates by returning to the desensitized state. As ACh concentration increases, the predominant closed component associated with closings within clusters becomes shorter as these closings reflect the set of transitions between unliganded closed and diliganded open states.⁴⁴

At 30 μM ACh, which is close to the EC_{50} of the muscle nAChR,⁴³ receptor activation was observed as opening events of 5 pA (-70 mV of membrane potential) grouped into clusters (Figure 3). Open duration histograms were fitted by a single exponential component of 1.10 ± 0.09 ms ($n = 6$ and $N = 5$) (Figure 3). Closed time distributions were described by three or four exponential components, of which the two briefest correspond to closings within clusters.^{31,44,45} Cluster duration was 145 ± 6 ms ($n = 6$ and $N = 5$), as described before.³¹ The main intracluster closed component showed a mean duration of 6.8 ± 0.7 ms ($n = 6$ and $N = 5$) (Figure 3).

We next compared the single-channel activity elicited by the different compounds. All recordings were performed in parallel with ACh recordings in the same batch of transfected cells as a control. In the presence of compounds 13, 14, 16, or 17, no channel activity was detected at either 100 μM ($n = 9$ and $N = 5$) or 500 μM ($n = 8$ and $N = 5$). We therefore discarded these compounds as agonists of muscle nAChR.

At 100 μM , compounds 12 and 15 and compounds 18 and 19 elicited channel activity, thus indicating their actions as agonists. The activation pattern for all of them differed from that observed with ACh as no clusters were distinguished, and openings appeared mainly isolated or in very short bursts, composed of one or two openings in quick succession (Figures 4 and 5). The frequency of channel activity and the kinetic properties differed among the different analogues.

Compound 18 behaved as a very low-efficacy agonist. At 100 μM , the low number of openings detected did not allow further

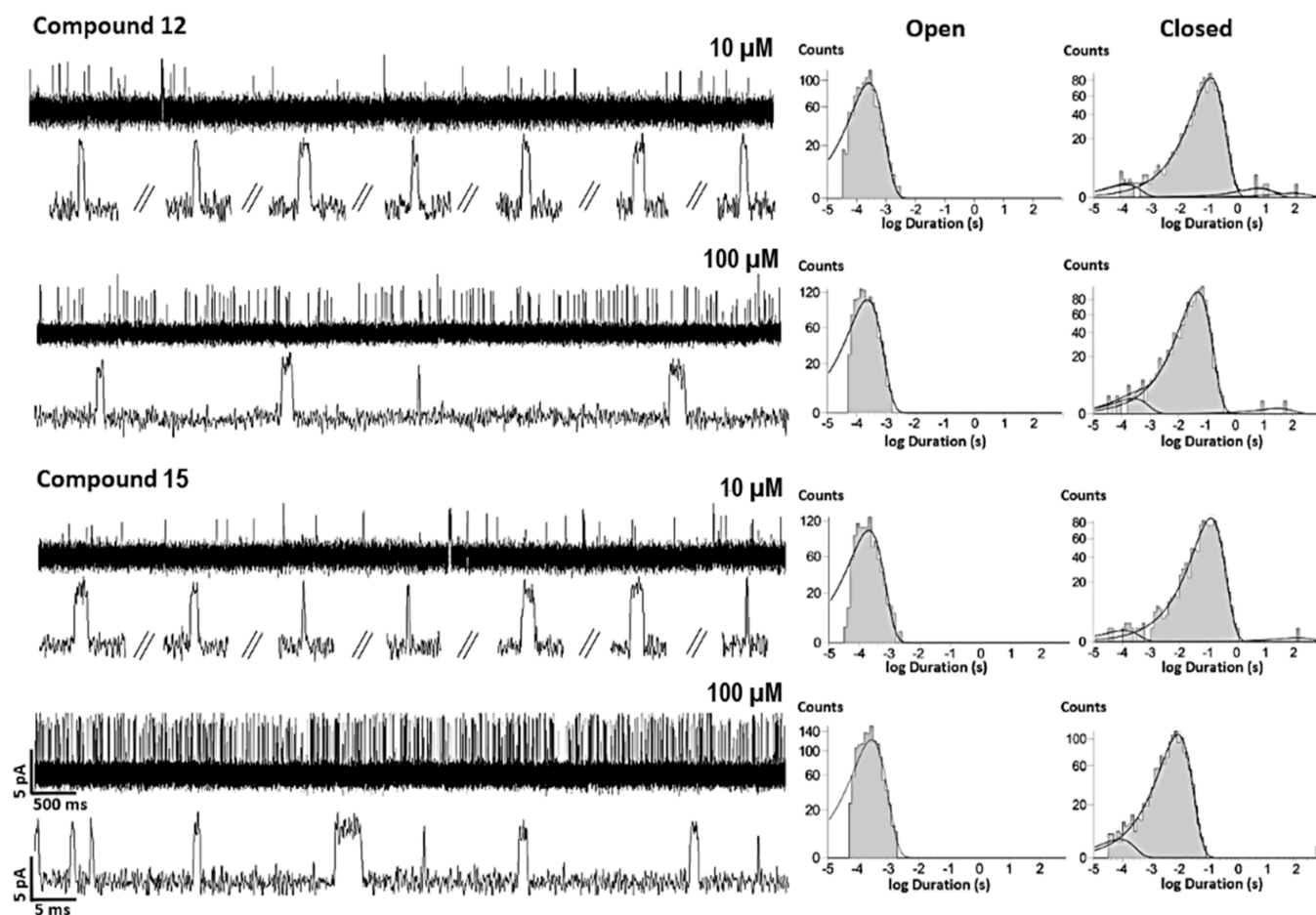


Figure 5. Muscle nAChR activation profile of **compounds 12 and 15** at 10 and 100 μM , recorded at -70 mV of membrane potential. Openings are shown as upward deflections. Representative open- and closed-duration histograms for each condition are shown on the right.

analysis ($n = 5$ and $N = 3$). At 500 μM ($n = 5$ and $N = 3$), channel activity was sufficient to generate open and closed time histograms. Open time histograms were fitted by a single component with a mean value of 0.11 ± 0.01 ms, indicating events significantly briefer than those activated by ACh ($p = 2.43 \times 10^{-6}$, comparison of mean values with Student t -test) (Figure 4). The main closed component showed a mean value of 165 ± 3.9 ms.

In the case of **compound 19**, which has the same substituent group but a linker with C5–NHC2, channel activity could be clearly detected at 100 μM . Channel openings were also briefer than those elicited by ACh, with a mean open time of 0.15 ± 0.01 ms. Closed time histograms were fitted by either two or three exponential components, and the mean duration of the main one was 61.9 ± 9 ms. At 500 μM ($n = 6$ and $N = 3$), the duration of the mean closed component was briefer than that at 100 μM , in line with the increase of channel activity (37.9 ± 3.5 ms, $p = 0.00163$ with respect to 100 μM). However, the mean open time was reduced to 0.08 ± 0.03 ms ($p = 3.9 \times 10^{-7}$, comparison of mean values with Student t -test) (Figure 4). The reduction of the mean open time by the increase of the compound concentration could be due to an open channel block as described for caffeine and **compound 9**.^{30,31}

In contrast to the low activity of the former analogues, high channel activity was detected with **compounds 12 and 15**. Although the frequency of openings was high in the presence of both compounds, clusters could not be distinguished. Channel activity was readily detected at 10 μM **compound 12**

concentration. The mean open time at 10 μM was 0.24 ± 0.01 ms, and the mean duration of the main closed component was 121 ± 2.6 ms ($n = 5$ and $N = 3$). Increasing the compound concentration to 100 μM did not affect mean open time, which was 0.24 ± 0.01 ms ($n = 5$ and $N = 3$, $p = 0.181$). However, the mean closed time decreased with respect to that at 10 μM (44.2 ± 6.2 ms; $p = 1.52 \times 10^{-5}$) (Figure 5).

A similar behavior was observed in **compound 15**, for which single-channel activity was detected at 10 μM . The mean open time was 0.25 ± 0.02 ms at 10 μM ($n = 5$ and $N = 3$) and 0.29 ± 0.02 ms at 100 μM ($n = 5$ and $N = 3$). The mean durations of the main closed component were 126.9 ± 6.9 ms at 10 μM and 7.4 ± 0.7 ms at 100 μM ($p = 3.5 \times 10^{-6}$, comparison of mean values with Student t -test) (Figure 5).

Independently of the efficiency, all of the compounds studied behaved as partial agonists of the muscle receptor, with an activation profile of isolated events without the ability to form clusters. These results are similar to those obtained with the previous analogues and also with the caffeine leader.^{30,31} In previous studies from our laboratory, we proposed that the length of the linker is not a determining factor in the structure of the analogue to trigger nAChR activity.³¹ This is in agreement with the results derived from the present work and clearly indicates that the partial agonist behavior of the analogues will depend mainly on the accessory group. Furthermore, although the new active synthesized analogues were less efficient than the previous one, they were more potent than caffeine.

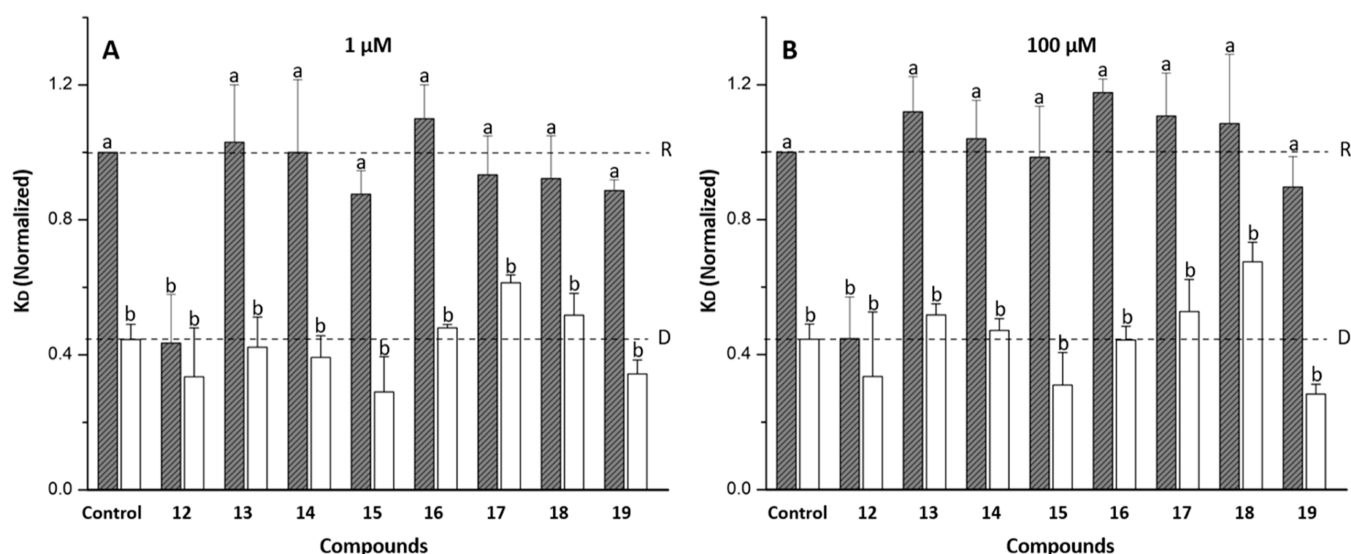


Figure 6. Normalized K_D values of CrV ($K_{D \text{ exp}}/K_{D \text{ rest}}$) in the absence and presence of carb (white and gray columns, respectively) obtained under the control condition or after incubation with two different concentrations [1 and 100 μ M, (A,B), respectively] of caffeine analogues (compounds 12–19). $K_{D \text{ rest}}$ corresponds to the K_D value obtained for control nAChR without carb. Each column represents the average \pm SD of the total number of samples under each condition; $n = 4$. Comparisons were made between each experimental condition and the control condition (with and without carb) and different letters (a–b) denote highly significant differences ($p < 0.01$).

Apart from the functional evaluation of these caffeine derivatives in nAChR activity, we performed studies to identify conformational changes induced by their presence. Previous studies have shown that caffeine and certain caffeine analogues with a linker of five or six carbon atoms between theophylline and pyrrolidine groups stabilized nAChR in its desensitized state, whereas theophylline alone or similar analogues with a linker of three or seven carbon atoms did not. However, all these molecules behaved as partial muscle nAChR agonists.^{30,31} In the present work, we analyzed possible conformational changes of nAChR in the presence of the new caffeine analogues. To this end, we used the crystal violet (CrV) fluorescent probe, a nAChR open-channel blocker which exhibits higher affinity for the desensitized (D) state compared to the resting (R) state.⁴⁶ Initially, nAChR-enriched *T. californica* membranes were incubated with synthesized caffeine analogues at concentrations of 1 and 100 μ M in the presence and absence of 1 mM carbamylcholine (carb). As experimental controls, membranes incubated with or without 1 mM carb were used. Differences in K_D values from samples before and after incubation with carb indicate different conformational states of the receptor and, indirectly, functional response of the nAChR to carb.^{30,31} We observed that, when caffeine analogues were incubated with carb, the K_D values were similar in all cases, indicating that receptor desensitization occurred (Figure 6). However, in the absence of carb, we observed that only compound 12 at 1 μ M ($n = 4$) and 100 μ M ($n = 4$) caused conformational changes of the nAChR, stabilizing it in a desensitized state (Figure 6). On the other hand, when the membranes were incubated with the rest of the analogues, no changes were observed with 1 μ M ($n = 4$) and 100 μ M ($n = 4$) as K_D values were similar to the control condition that corresponds to the resting state (Figure 6).

With patch clamp experiments, we observed that compounds 13, 14, 16, and 17 did not activate the receptor, being therefore expected that they could not cause protein conformational changes. Compound 12, with a linker of 5 C atoms, behaved similar to what was observed previously with compound 9, i.e., stabilization of the nAChR desensitization conformation.

However, compound 18 was observed to behave as a partial agonist of the nAChR and has a linker of five carbons, but it did not stabilize a desensitized conformation. The only difference between this analogue and compounds 9 and 12 is the presence of a N atom of the linker. Thus, although compound 18 was found to be less efficient than compound 9, it did not stabilize the receptor in a nonactive conformation. This can be considered to be a gain of function. Finally, compounds 15 and 19, with linkers of seven C atoms, activated the receptor and behaved similar to what was observed previously with compound 11, i.e., without stabilization of the nAChR desensitization conformation.

These results indicate that the agonist behavior depends on the accessory group of the compounds, whereas stabilization in a desensitized state depends on either the interactions of the linker at the binding site or the different interactions that the theophylline group forms with distinct linkers (longer linkers or those containing an N atom).

In Silico Binding of Synthetic Caffeine Analogues to nAChR. To evaluate the molecular interactions between nAChR and caffeine analogues that showed nAChR activation and produced different conformational changes in nAChR, we performed molecular docking studies using the structure of the muscle-type nAChR from *T. californica* in complex with nicotine (7QL5.pdb).⁴⁷ The muscle nAChR has two orthosteric sites formed by the extracellular domain of two adjacent subunits, corresponding to the $\alpha 1/\delta$ and $\alpha 1/\gamma$ interfaces. These interfaces are virtually superimposable. Both sites have similar geometries and are formed by a principal face (α subunit) involving loops A, B, and C and a complementary face with loops D, E, and F (non- α subunit).⁴⁷

Full agonists and partial agonists lead to a different stabilization of the C loop of α subunit: in the case of full agonists, they totally close this loop which looks like a cap of the binding pocket,⁴⁸ whereas some partial agonists cannot induce a complete closing of the C loop (i.e., causing a partial response of the channel).^{49,50} Nicotine, like carb, is an activator of nAChR with a higher activating potency for neuronal nAChR receptors

Table 3. Binding Energy and Interacting Residues of Docking Studies with the Muscle-Type nAChR from *T. californica*^a

	BBE (Kcal/mol)	Interacting residues												
Nicotine	-6,3	W57	Y93	L111	L121	Y190	C192	C193	Y198					
Compound 12	-8.1	W57	D59	Y93	L111	R113	L121	W149	Y190	C192	C193	Y198		
Compound 15	-7.5	W57	D59	Y93	L111	R113	T119	L121	W149	Y190	C192	C193	Y198	
Compound 18	-8.5	W57	D59	Y93	L111	R113	T119	L121	W149	Y190	C192	C193	Y198	
Compound 19	-8.0	W57	D59	Y93	L111	R113	T119	L121	W149	T150	Y190	C192	C193	Y198

^aThe BBE of the most stable conformation obtained after docking analyses is shown for each ligand. All the interacting residues observed in the different conformations are listed for each ligand (interacting residues identified for previous synthesized compounds in black⁵²). Data correspond to 10 independent docking experiments.

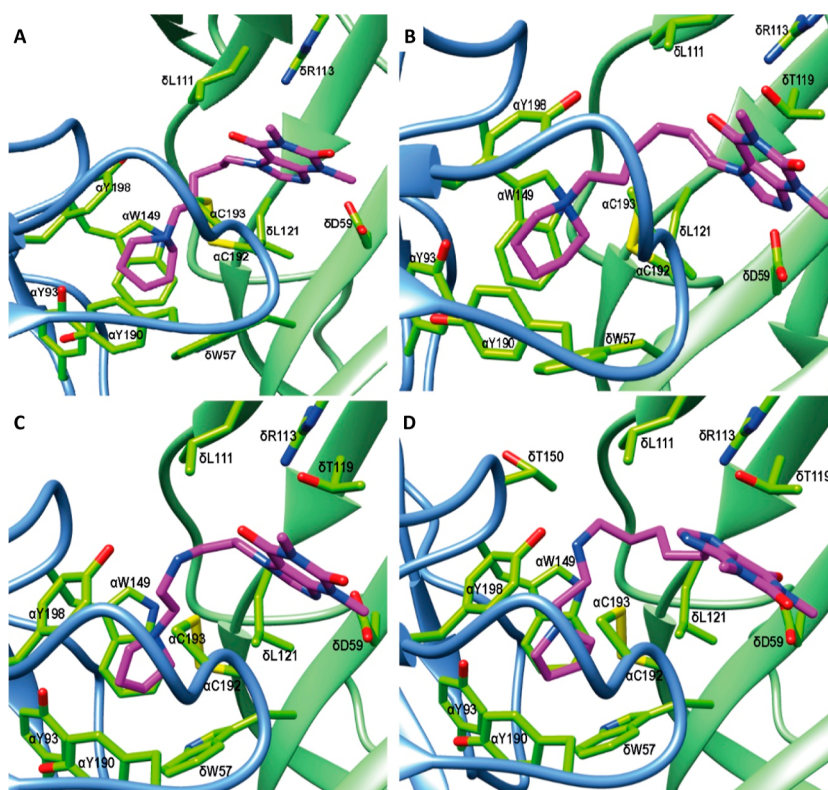


Figure 7. Molecular docking into the agonist-binding site of the muscle-type nAChR from *T. californica*. Close-up view of the caffeine analogues bound at the α/δ interface: (A) compound 12, (B) compound 15, (C) compound 18, and (D) compound 19. Caffeine analogues are shown as violet sticks, the surrounding residues in the binding site are shown as green sticks, and α and δ AChR subunit backbones are shown as blue and green sticks, respectively.

than for muscle receptors.^{47,51,52} This difference can be explained through the different position that some amino acids adopt depending on nicotine presence. Thus, whereas at the active site some important amino acids adopt similar geometries for both receptors, others adopt different geometries.⁴⁷ Therefore, the low affinity of nicotine for muscle nAChR could be due to differences in the electrostatic environment of the active site that prevent the stabilization of the C-loop in a closed state. Nicotine could thus be considered a partial agonist of muscle receptors.

Taking into account that electrophysiological studies showed that compounds 12, 15, 18, and 19 activate the receptor

possibly through partial agonism, we carried out docking studies with the structure of the muscle nAChR (*T. californica*) obtained in complex with nicotine. First, we docked nicotine to the $\alpha1/\delta$ orthosteric site of the nAChR using the 7QL5.pdb structure and performing 10 independent assays. The main conformation obtained showed similar interactions to those already reported⁴⁷ with a score of approximately -6.3 kcal/mol. H-bridge interaction was observed with $\alpha Y198$, which could stabilize nicotine ammonium, and hydrophobic interactions were observed with $\delta L111$, $\delta L121$, $\delta W57$, $\alpha Cys192$, $\alpha Cys193$, $\alpha Y93$, and $\alpha Y190$ (Figure S2 and Table 3). All these residues are a part of the orthosteric binding pocket of nAChR.^{48–50}

Then, using the same protocol, we carried out the docking with active **compounds 12, 15, 18, and 19**. All of the compounds analyzed showed the ability to interact with residues from both the main and the complementary faces of the agonist site. The binding scores were found within a range between -7.5 and -8.5 kcal/mol (Table 3). In all cases, the theophylline group was located in the outermost part of the binding pocket, whereas the pyrrole and piperidine groups were oriented toward the innermost part (Figure 7). Theophylline groups formed H-bridge with $\delta R113$ and hydrophobic interactions with $\delta R113$, $\alpha C192$, and $\alpha C193$. In addition to these interactions, the theophylline groups of **compounds 12 and 15** formed cation– π with $\delta R113$ and hydrophobic interactions with $\delta D59$ and $\delta L111$, and the theophylline group of **compound 19** analogue interacted through a salt bridge with $\delta D59$ (Figure 7 and Table 3). On the other hand, the pyrrole and piperidine groups established H-bridge and π -cation interactions with $\alpha W149$ and hydrophobic interactions with $\alpha W57$, $\alpha Y93$, $\alpha W149$, and $\alpha Y190$. The piperidine group also formed hydrophobic interactions with $\alpha Y198$ (Figure 7 and Table 3). As it is highlighted in Table 3, similar interactions were observed between the pyrrole group and the caffeine analogues studied in our previous research.³¹

Similar to what was observed in the docking of these compounds with AChE, in the present study, a higher amount of hydrophobic interactions were also observed with the analogues either having the C7 linker or containing an amine group, compared to the analogues with C5 linker. While the linkers of all the compounds studied showed hydrophobic interactions with $\delta L111$ and $\delta L121$ residues, the linker of **compound 15** also formed hydrophobic interactions with $\delta T119$ and $\alpha Y198$ residues and the linkers of **compounds 18 and 19** also established hydrophobic interactions with $\delta T119$, $\delta L111$, and $\alpha Y198$, and, in addition, the amino group of both linkers formed an H-bridge with $\alpha Y198$ (Figure 7 and Table 3). The linker of **compound 19** also formed hydrophobic interactions with $\alpha T150$ and $\delta Leu121$.

Although nAChR conformation studies with the CrV probe showed that of all the active caffeine derivatives only **compound 12** led the receptor to a desensitized state, molecular docking studies did not show any different interactions among these compounds. We thus worked with a resting-state nAChR to simulate the initial interactions between the analogues and the nAChR. We therefore repeated docking studies using a recently published *T. californica* nAChR model (7QKO.pdb).⁴⁷ Although mostly similar interactions were observed for all compounds and similar to those described above, only the theophylline group of **compound 12** formed an H-bridge with $\alpha Y198$.

In spite of the similarities and differences in the interactions that were reported for the previously synthesized caffeine analogues,³¹ all caffeine analogues that activated the nAChR did so through their ability to interact with key orthosteric site residues that are critical for their pharmacological function and that explain their behavior as partial agonists.⁴⁷ Figure 8 summarizes the most relevant pharmacophore characteristics of nAChR partial activation, which are deduced from the results presented herein.

Concludingly, our study documents a new group of synthesized caffeine analogues that show AChE inhibition and that behave in different manners against muscle AChR. Not all of them did activate nAChR and those that did showed differences in activity and in nAChR conformation stabilization. Although

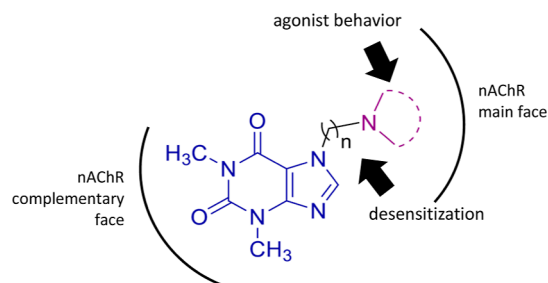


Figure 8. Schematic diagram summarizing the most relevant pharmacophore characteristics of nAChR partial activation and desensitization resulting from caffeine derivatives.

this new group of molecules—compared to those previously studied in our lab— did not improve their action on nAChR, several of them did improve AChE inhibitory potency. We therefore propose **compound 19** as a new promising leader for further studies because it not only shows a high AChE inhibitory potency, which is comparable to tacrine, but also behaves as a partial agonist of muscle nAChR without causing receptor desensitization which results in a further potentiation of the cholinergic system. Taken together, all of these results give valuable information about the necessary pharmacophoric chemical properties for both nAChR and AChE molecular targets.⁵⁶

MATERIALS AND METHODS

All of the chemicals used were of the best available grade (Aldrich, Merck) and were employed without further purification. DMF was dried by keeping it over 4A molecular sieves under a nitrogen atmosphere. AChE from electric eel (type VI–S), 5,5'-dithiobis(2-nitrobenzoic acid) (DTNB) and acetylthiocholine iodide and all other drugs were obtained from Sigma-Aldrich.

Microwave-assisted reactions were carried out in a CEM Discover Benchmate reactor programmable up to 300 W, using 10 mL closed vials, with a magnetic stirrer. The temperature of the equipment was monitored and controlled by an infrared sensor (programmable between 25 and 250 °C). The DMF reaction solvent was dried by keeping it over 4A molecular sieves under a nitrogen atmosphere.

¹H and ¹³C NMR spectra including correlation spectroscopy, heteronuclear single-quantum coherence (HSQC), and heteronuclear multiple-bond correlation experiments were recorded on a Bruker Avance ARX-300 spectrophotometer at room temperature in chloroform-D1 or methanol-D4. Chemical shifts (δ) are reported in parts per million (ppm) from tetramethylsilane ($\delta = 0.00$ ppm).

Column chromatography was carried out with Merck silica gel 60 (0.2–0.63 mm, 240–400 mesh). The reaction progress was monitored using silica gel-60 F 254 chromatofolios (Merck). Thin-layer chromatograms were developed with an appropriate mobile phase and visualized with UV light (254 nm).

All derivatives were rigorously characterized by NMR spectroscopy. For the new compounds, copies of ¹H, ¹³C, DEPT, and HSQC NMR graphical spectra are also provided (Figure S3A–O).

High-resolution mass spectrometry with electrospray ionization (HRMS-ESI) data in positive mode were acquired by using a BRUKER micrOTOF-Q II instrument. The sample solution, consisting of methanol and formic acid, underwent analysis with the following instrument parameters: nebulizer at 3.5 bar, capillary set to 4000 V, dry heater maintained at 200 °C, and dry gas flow set at 7.0 L/min. Mass scanning covered the range from 70 to 1000 *m/z*, with a plate offset of -500 V and a collision cell RF of 300.0 Vpp.

Synthesis of Caffeine Analogues. General Procedure for the Synthesis of Alkylbrominated Intermediates 2–4. Alkylbrominated intermediates were synthesized using theophylline as the starting reagent and the corresponding dibromoalkane (1,3-dibromopropane,

1,5-dibromopentane, and 1,7-dibromoheptane) as previously reported³¹ (Scheme 1).

General Procedure for the Synthesis of Compounds 12–17. A mixture of an alkylated compound 3–4 (0.1 mmol) and the corresponding amine (piperidine, diethylamine, or 1-methylpiperazine, 0.3 mmol) in anhydrous DMF (1 mL) was placed in a special vial for the microwave reaction. The solution was irradiated (100 °C, 150 W) for 10–30 min until the disappearance of the starting compound was verified by TLC. The solvent was removed by adding distilled H₂O (5 mL), and the desired compound was extracted with dichloromethane (3 × 2 mL). The organic phase was dried over anhydrous Na₂SO₄ and filtered, and the solvent was evaporated to afford the desired product (Scheme 1). For compounds 15–17, it was necessary to perform a purification by column chromatography on silica gel high-purity grade (pore size 60 Å, 230–400 mesh particle size) with dichloromethane/methanol to obtain the pure desired product.

1,3-Dimethyl-7-(5-(piperidin-1-yl)pentyl)-1H-purine-2,6(3H,7H)-dione (Compound 12). Yellow oil (74% yield). ¹H NMR (300 MHz, CDCl₃) δ 7.52 (s, 1H), 4.25 (t, *J* = 7.1 Hz, 2H), 3.56 (s, 3H), 3.38 (s, 3H), 2.31 (s, 4H), 2.23 (t, *J* = 7.7 Hz, 2H), 1.86 (p, *J* = 7.4 Hz, 2H), 1.52 (h, *J* = 7.1, 6.3 Hz, 6H), 1.39 (q, *J* = 5.7 Hz, 2H), 1.27 (p, *J* = 8.4 Hz, 2H). ¹³C NMR (75 MHz, CDCl₃) δ: 155.17, 151.77, 149.00, 140.92, 107.03, 59.19, 54.71, 47.29, 30.85, 29.85, 28.07, 26.40, 26.01, 24.50. HRMS-ESI *m/z*, calcd for [M + H]⁺: 334.2238; found, 334.2233.

7-(5-(Diethylamino)pentyl)-1,3-dimethyl-1H-purine-2,6(3H,7H)-dione (Compound 13). Brown oil, (71% yield). ¹H NMR (300 MHz, CDCl₃) δ 7.67 (s, 1H), 4.31 (s, 2H), 3.57 (s, 3H), 3.38 (s, 3H), 3.15 (s, 4H), 3.04–2.93 (m, 2H), 2.01–1.89 (m, 4H), 1.41 (t, *J* = 7.3 Hz, 8H). ¹³C NMR (75 MHz, CDCl₃) δ: 155.17, 151.66, 149.07, 141.41, 106.87, 51.32, 46.63, 46.47, 30.13, 29.85, 28.03, 23.41, 22.83, 8.57. HRMS-ESI *m/z*, calcd for [M + H]⁺: 322.2238; found, 322.2239.

1,3-Dimethyl-7-(5-(4-methylpiperazin-1-yl)pentyl)-1H-purine-2,6(3H,7H)-dione (Compound 14). Yellow oil (59% yield). ¹H NMR (300 MHz, CDCl₃) δ 4.24 (s, 1H), 3.55 (s, 3H), 3.36 (s, 3H), 2.48 (s, 7H), 2.38–2.27 (m, 6H), 1.86 (p, *J* = 7.5 Hz, 3H), 1.52 (p, *J* = 7.5 Hz, 3H), 1.30 (q, *J* = 8.0 Hz, 3H). ¹³C NMR (75 MHz, CDCl₃) δ: 155.15, 151.73, 149.00, 140.90, 107.00, 58.11, 54.83, 52.90, 47.22, 45.87, 30.79, 29.83, 28.06, 26.12, 24.28. HRMS-ESI *m/z*, calcd for [M + H]⁺: 349.2347; found, 349.2331.

1,3-Dimethyl-7-(7-(piperidin-1-yl)heptyl)-1H-purine-2,6(3H,7H)-dione (Compound 15). Yellow oil (68% yield). ¹H NMR (300 MHz, CDCl₃) δ 7.56 (s, 1H), 4.22 (t, *J* = 7.1 Hz, 2H), 3.53 (s, 3H), 3.34 (s, 3H), 3.06 (s, 3H), 2.93–2.81 (m, 2H), 2.02 (s, 4H), 1.82 (q, *J* = 7.5 Hz, 4H), 1.63 (s, 2H), 1.38–1.18 (m, 6H). ¹³C NMR (75 MHz, CDCl₃) δ: 155.08, 151.68, 148.94, 141.06, 106.89, 57.40, 53.22, 47.15, 30.68, 29.78, 28.24, 27.99, 26.49, 25.92, 23.41, 22.58, 22.09. HRMS-ESI *m/z*, calcd for [M + H]⁺: 362.2551; found, 362.2546.

7-(7-(Diethylamino)heptyl)-1,3-dimethyl-1H-purine-2,6(3H,7H)-dione (Compound 16). Brown oil, (71% yield). ¹H NMR (300 MHz, CDCl₃) δ 7.51 (s, 1H), 3.98 (s, 5H), 3.56 (s, 3H), 3.21–3.05 (m, 4H), 3.04–2.92 (m, 2H), 1.92–1.73 (m, 2H), 1.72–1.54 (m, 2H), 1.46–1.33 (m, 12H).

¹³C NMR (75 MHz, CDCl₃) δ: 155.24, 151.44, 148.69, 141.40, 107.63, 51.12, 46.57, 41.11, 33.58, 29.66, 28.57, 27.70, 26.64, 26.56, 23.02, 8.65. HRMS-ESI *m/z*, calcd for [M + H]⁺: 350.2551; found, 350.2556.

1,3-Dimethyl-7-(7-(4-methylpiperazin-1-yl)heptyl)-1H-purine-2,6(3H,7H)-dione (Compound 17). Yellow oil (52% yield). ¹H NMR (300 MHz, CDCl₃) δ 7.51 (s, 1H), 4.21 (t, *J* = 7.2 Hz, 2H), 3.52 (s, 3H), 3.34 (s, 3H), 2.77 (s, 8H), 2.51–2.44 (m, 2H), 2.42 (s, 3H), 1.88–1.72 (m, 2H), 1.52 (s, 2H), 1.27 (s, 6H). ¹³C NMR (75 MHz, CDCl₃) δ: 155.14, 151.73, 148.98, 140.94, 106.98, 57.79, 53.46, 51.55, 47.28, 45.01, 30.84, 29.83, 28.72, 28.05, 26.99, 26.22, 25.59. HRMS-ESI *m/z*, calcd for [M + H]⁺: 377.2660; found, 377.2662.

General Procedure for the Synthesis of Compounds 18 and 19. To obtain derivatives 5 and 6, the alkylbrominated intermediate (2 and 4, 0.1 mmol) was reacted with 2-(pyrrolidin-1-yl)ethanamine (0.3 mmol) in anhydrous DMF (2 mL) (Scheme 2). The reaction was carried out conventionally at room temperature for 4 h and was monitored every hour by TLC.

1,3-Dimethyl-7-(3-((2-(pyrrolidin-1-yl)ethyl)amino)propyl)-1H-purine-2,6(3H,7H)-dione (Compound 18). Yellow oil (77% yield). ¹H NMR (300 MHz, CDCl₃) δ: 7.60 (s, 1H), 4.39 (t, *J* = 6.8 Hz, 2H), 3.57 (s, 3H), 3.39 (s, 3H), 2.70 (t, *J* = 5.9 Hz, 2H), 2.63–2.56 (m, 4H), 2.53 (q, *J* = 6.6 Hz, 4H), 2.03 (p, *J* = 6.7 Hz, 3H), 1.78 (p, *J* = 3.2 Hz, 4H). ¹³C NMR (75 MHz, CDCl₃) δ: 155.23, 151.83, 149.08, 141.58, 107.01, 56.01, 54.34, 48.42, 46.11, 45.01, 30.88, 29.89, 28.10, 23.54. HRMS-ESI *m/z*, calcd for [M + H]⁺: 335.2190; found, 335.2197.

1,3-Dimethyl-7-(5-((2-(pyrrolidin-1-yl)ethyl)amino)pentyl)-1H-purine-2,6(3H,7H)-dione (Compound 19). Yellow oil (37% yield). ¹H NMR (300 MHz, CDCl₃) δ 7.52 (s, 1H), 4.27 (t, *J* = 7.1 Hz, 2H), 3.57 (s, 3H), 3.39 (s, 3H), 2.69 (t, *J* = 6.2 Hz, 2H), 2.58 (q, *J* = 7.3, 6.6 Hz, 4H), 2.47 (p, *J* = 4.2, 3.4 Hz, 4H), 1.88 (p, *J* = 7.4 Hz, 4H), 1.74 (p, *J* = 3.2 Hz, 4H), 1.52 (p, *J* = 7.3 Hz, 2H), 1.34 (p, *J* = 7.4, 6.6 Hz, 2H). ¹³C NMR (75 MHz, CDCl₃) δ: 155.21, 151.81, 149.05, 140.94, 107.07, 56.10, 54.36, 49.94, 48.76, 47.34, 30.93, 29.88, 29.65, 28.11, 24.27, 23.56. HRMS-ESI *m/z*, calcd for [M + H]⁺: 363.2503; found, 363.2511.

AChR-Rich Membrane Preparation. AChR-rich membranes were obtained from a *T. californica* specimen's electric tissue from the Pacific Coast of California (Aquatic Research Consultants, San Pedro, CA, USA), as previously described.⁵⁷ This electric tissue was cut into small pieces, homogenized using a Virtis homogenizer under controlled conditions, and subjected to a series of centrifugation steps, followed by a high-speed sucrose gradient centrifugation. The middle fraction obtained corresponds to AChR-rich membranes with a specific activity averaging 1.0–1.5 nmol α-BTX sites/mg protein.⁵⁷ Samples containing nAChR-rich membranes were subsequently stored at –20 °C before being used.

Cell Culture. BOSC 23 cells derived from the HEK 293 line (provided by Dr. Sine, Mayo Clinic, USA) were cultured in Dulbecco's modified Eagle medium (DMEM) (GIBCO, USA) supplemented with 100 μg/mL streptomycin, 100 IU/mL penicillin (Invitrogen, USA), and 10% fetal bovine serum (Internegeocios, Argentina) in a 5% CO₂ atm at 37 °C.

Receptor Expression. BOSC-23 cells were transfected with mouse α, β, δ, and ε subunit cDNAs (for the adult muscle nAChR, α1, β1δε) in a 2:1:1:1 ratio, as previously described.⁴⁵ A plasmid-encoding green fluorescent protein was included in all transfections for the identification of transfected cells under fluorescence optics. Cells were left in contact with a calcium phosphate-DNA precipitate for 14–18 h. DMEM medium was subsequently changed, and cells were incubated for a further 24–48 h long period to allow receptor expression.³¹

In Vitro AChE Activity Evaluation. AChE activity was evaluated following Ellman's methodology with slight modifications.⁵⁸ Briefly, 300 μL of enzyme solution (0.126 U/mL prepared by dilution with buffer B—8 mM K₂HPO₄, 2.3 mM NaH₂PO₄, 0.15 M NaCl, 0.05% Tween 20, pH 7.6—of a stock solution of 5 U/mL prepared in buffer A—8 mM K₂HPO₄, 2.3 mM NaH₂PO₄) was incubated with 300 μL of each compound solution (dissolved in buffer B plus 2.5% MeOH as a cosolvent) at room temperature for 60 min. The reaction was started by the addition of 600 μL of the substrate solution [0.5 mM 5'-dithio-bis(2-nitrobenzoic acid, DTNB), 0.6 mM acetylthiocholine iodide (ATCh), 0.1 M Na₂HPO₄, pH 7.5], and absorbance was measured at 405 nm for 120 s at 25 °C (JASCO V-630BIO spectrophotometer equipped with an EHCS-760 Peltier; Tokyo, Japan). AChE activity evaluation is based on the ability of AChE to hydrolyze the substrate ATCh to produce thiocholine, which then reacts with the chromogenic reagent DTNB to produce a yellow-colored product, 2-nitro-5-thiobenzoic acid (TNB). The rate of TNB formation is directly proportional to AChE activity. AChE activity was obtained by comparing the reaction rates of the samples and the blank. Nonlinear regression analysis was used to determine the sample concentration that resulted in 50% inhibition (IC₅₀) by plotting the response curve against the logarithm of the concentration using GraphPadPrism 5. Tacrine was used as a reference inhibitor in this assay. All the experiments were performed in triplicate.

Electrophysiological Experiments. BOSC-23 cells expressing muscle AChR were used for single-channel measurements 2 days after transfection. Single-channel recordings were performed in the cell-

attached patch clamp configuration at room temperature ($\sim 20^\circ\text{C}$) and at -70 mV membrane potential. Extracellular solution and pipet solutions contained 142 mM KCl, 5.4 mM NaCl, 1.8 mM CaCl_2 , 1.7 mM MgCl_2 , and 10 mM HEPES (pH 7.4).⁵⁹ ACh or caffeine analogues were added to the pipet solution. Single-channel currents were recorded using an Axopatch 200 B patch clamp amplifier (Axon Instruments, Inc., CA), digitized at 5–10 μs intervals using the program Acquire (Bruyton Corporation, Seattle, WA) and detected by the half amplitude threshold criterion using the program TAC (Bruyton Corporation, Seattle, WA) at a final bandwidth of 9 kHz. Open and closed time histograms were plotted using a logarithmic abscissa and a square-root ordinate and fitted to the sum of exponentials by maximum likelihood using the program TACFit (Bruyton Corp., Seattle, WA). Clusters were identified as a series of closely spaced events preceded and followed by closed intervals of >2 h longer than a specified duration (tcrit). This duration was taken as the point of intersection of the predominant closed time component and the succeeding one in the closed time histogram.^{43–45,59} Cluster duration was taken from the longest-duration component of the open time histogram constructed with an imposed tcrit.

nAChR Conformational-State Characterization. To understand the molecular mechanism underlying AChR activation by synthetic caffeine analogues, we evaluated the nAChR conformational state after incubation with caffeine analogues. nAChR-rich membranes were resuspended in buffer A (150 mM NaCl, 0.25 mM MgCl_2 , and 20 mM HEPES buffer, pH 7.4) at a final concentration of 100 μg protein/mL. nAChR conformational changes were assessed using crystal violet (CrV), a nAChR channel open blocker, as previously described.^{30,31,60} nAChR-rich membranes resuspended in buffer A were incubated with each caffeine analogue for 15 min. When measurements were made with nAChR in the desensitized state, nAChR-rich membranes were previously incubated with 1 mM carbamylcholine (carb) for 15 min. Membranes were subsequently titrated at increasing concentrations of CrV (in buffer A). After each CrV addition, the samples were incubated for 15 min before fluorescence emission spectra were obtained. CrV was excited at 600 nm, and fluorescence emission spectra were collected from 605 to 700 nm. Before the first addition of CrV, a background fluorescence emission spectrum was obtained for each sample. These spectra were then subtracted from the emission spectra obtained in the presence of CrV, and the maximum intensity (at 623–625 nm) was measured. To determine CrV dissociation constants (K_D), CrV peak fluorescence emission values were plotted as a function of \log CrV (M) concentrations. The resulting sigmoid curve was fitted to the Boltzmann function, and K_D value was obtained. Fluorimetric measurements were performed in 1.0 mL quartz cuvettes on an SLM model 4800 fluorimeter (SLM Instruments, Urbana, IL) using a Hannoveria 200-W mercury/xenon arc vertically polarized beam obtained with a Glan-Thompson polarizer (4 nm excitation and emission slits).

Molecular Docking. In order to further understand the interactions between caffeine analogues and nAChR or AChE, we performed molecular docking studies. For *in silico* studies, we used the following structures from the Protein Data Bank (PDB): muscle-like nAChR from *T. californica* in a nicotine-bound conformation (PDB code 7QLS)⁴⁷ and human AChE (PDB code 4EY7).³⁶ Ligands were designed with Avogadro 1.2.0 and coupled with Chimera 1.16 (Chimera UCSF Resource for Biocomputing, Visualization, and Informatics; www.rbvi.ucsf.edu/chimera).⁶¹ We performed molecular docking simulations using the AutoDock Vina 1.1.2 software^{62,63} via UCSF Chimera 1.16.⁶¹ Prior to the docking experiments, we meticulously prepared the protein–ligand systems. Water molecules were removed, and hydrogen atoms were added to the protein and ligand structures at a pH of 7.4. Gasteiger charges were assigned, and default parameters were maintained for the remaining settings. The grid was defined around the orthosteric binding site of the nAChR models and at the CAS/PAS site of the AChE structure. One hundred genetic algorithm runs were performed for each condition. The docking results were further corroborated through a series of six distinct procedures. To visualize the most representative docking result, we used Chimera 1.16. Protein–ligand interactions were analyzed using LIGPLOT v.4.5.3^{64,65}

and Protein Ligand Interaction Profiler (PLIP)⁶⁶ (<https://plip-tool.biotec.tu-dresden.de/plip-web/plip/>).

Data Analysis. In CrV fluorescent experiments and AChE activity evaluation, a comparison of more than two mean values was made by analysis of variance (randomized one-way ANOVA), followed by post hoc test analysis of Bonferroni multiple comparisons. Differences were considered significant at $p < 0.05$ and highly significant at $p < 0.01$. In the case of $n = 3$, data were considered if the coefficient of variation (standard deviation/mean) was <0.1 . When comparison of two mean values was performed, as in electrophysiological experiments, unpaired Student's *t*-test was used.

■ ASSOCIATED CONTENT


● Supporting Information

The Supporting Information is available free of charge at <https://pubs.acs.org/doi/10.1021/acscchemneuro.3c00710>.

Molecular docking into the CAS/PAS site of the human AChE (4EY7.pdb), 3D structure of AChE showing the best donepezil conformation, and detailed 3D binding mode of donepezil and tacrine; molecular docking into the agonist binding site of the muscle-type nAChR from *T. californica* in complex with nicotine (7QLS.pdb), 3D structure of nAChR showing the best conformation bound for nicotine, and close-up view of nicotine bound at the α/δ interface; and ^1H NMR (300 MHz) and ^{13}C NMR (75 MHz) spectra in CDCl_3 of **12**, DEPT 135 (75 MHz) spectra in CDCl_3 of **12**, ^1H NMR (300 MHz) and ^{13}C NMR (75 MHz) spectra in CDCl_3 of **13**, DEPT 135 (75 MHz) NMR and HSQC NMR spectra in CDCl_3 of **13**, ^1H NMR (300 MHz) and ^{13}C NMR (75 MHz) spectra in CDCl_3 of **14**, DEPT 135 (75 MHz) NMR and HSQC NMR spectra in CDCl_3 of **14**, ^1H NMR (300 MHz) and ^{13}C NMR (75 MHz) spectra in CDCl_3 of **15**, DEPT 135 (75 MHz) NMR and HSQC NMR spectra in CDCl_3 of **15**, ^1H NMR (300 MHz) and ^{13}C NMR (75 MHz) spectra in CDCl_3 of **16**, ^1H NMR (300 MHz) and ^{13}C NMR (75 MHz) spectra in CDCl_3 of **17**, DEPT 135 (75 MHz) NMR and HSQC NMR spectra in CDCl_3 of **17**, ^1H NMR (300 MHz) and ^{13}C NMR (75 MHz) spectra in CDCl_3 of **18**, (M) DEPT 135 (75 MHz) NMR and HSQC NMR spectra in CDCl_3 of **18**, ^1H NMR (300 MHz) and ^{13}C NMR (75 MHz) spectra in CDCl_3 of **19**, and DEPT 135 (75 MHz) NMR and HSQC NMR spectra in CDCl_3 of **19** (PDF)

■ AUTHOR INFORMATION

Corresponding Author

Silvia Antollini — Instituto de Investigaciones Bioquímicas de Bahía Blanca, Departamento de Biología, Bioquímica y Farmacia, Universidad Nacional del Sur and Consejo Nacional de Investigaciones Científicas y Técnicas, Bahía Blanca 8000, Argentina;  orcid.org/0000-0002-4655-1292; Email: silviant@criba.edu.ar

Authors

Juan Pablo Munafó — Instituto de Investigaciones Bioquímicas de Bahía Blanca, Departamento de Biología, Bioquímica y Farmacia, Universidad Nacional del Sur and Consejo Nacional de Investigaciones Científicas y Técnicas, Bahía Blanca 8000, Argentina

Brunella Biscussi — Instituto de Química del Sur, Departamento de Química, Universidad Nacional del Sur and Consejo

Nacional de Investigaciones Científicas y Técnicas, Bahía Blanca 8000, Argentina

Diego Obiol – Grupo de Biofísica, Instituto de Física del Sur, Departamento de Física, Universidad Nacional del Sur and Consejo Nacional de Investigaciones Científicas y Técnicas, Bahía Blanca 8000, Argentina

Marcelo Costabel – Grupo de Biofísica, Instituto de Física del Sur, Departamento de Física, Universidad Nacional del Sur and Consejo Nacional de Investigaciones Científicas y Técnicas, Bahía Blanca 8000, Argentina

Cecilia Bouzat – Instituto de Investigaciones Bioquímicas de Bahía Blanca, Departamento de Biología, Bioquímica y Farmacia, Universidad Nacional del Sur and Consejo Nacional de Investigaciones Científicas y Técnicas, Bahía Blanca 8000, Argentina; orcid.org/0000-0003-0388-6129

Ana Paula Murray – Instituto de Química del Sur, Departamento de Química, Universidad Nacional del Sur and Consejo Nacional de Investigaciones Científicas y Técnicas, Bahía Blanca 8000, Argentina

Complete contact information is available at:

<https://pubs.acs.org/10.1021/acschemneuro.3c00710>

Author Contributions

Juan Pablo Munafó: conceptualization; investigation; validation; and writing—original draft. **Brunella Biscussi**: conceptualization; investigation; validation; and writing—original draft. **Diego Obiol**: investigation and visualization. **Marcelo Costabel**: supervision. **Cecilia Bouzat**: conceptualization; supervision; funding acquisition; and writing—review and Editing. **Ana Paula Murray**: conceptualization; supervision; funding acquisition; and writing—review and editing. **Silvia Susana Antollini**: conceptualization; supervision; project administration; funding acquisition; writing—original draft; and writing—review and editing. J.P.M. and B.B. authors contributed equally to this work.

Notes

The authors declare no competing financial interest.

ACKNOWLEDGMENTS

We are grateful to Translator Viviana Soler for her diligent work in editing this article. This work has been supported by *Agencia Nacional de Promoción de la Investigación, el Desarrollo Tecnológico y la Innovación* (ANPIDTYI) (PICT 2019-02687 to SSA; PICT 2020-00936 to C.B.; and PICT2020-01187 to A.P.M.), *Universidad Nacional del Sur* (PGI 24/B282 to SSA; PGI 24/B298 to C.B.; and PGI 24/Q105 to A.P.M.), and *Consejo Nacional de Investigaciones Científicas y Técnicas* (CONICET) (PIP11220200102356 to C.B. and PIP 11220200100834CO to A.P.M.), Argentina.

ABBREVIATIONS

ACh, acetylcholine; AChE, acetylcholinesterase; AChR, acetylcholine receptor; ATCh, acetylthiocholine; AD, Alzheimer's disease; BBE, best binding energy; α -BTX, α -bungarotoxin; Carb, carbamylcholine; ^{13}C , carbon-13; CAS, catalytic site; CDCl_3 , chloroform- d ; CrV, crystal violet; D, desensitized state; DMF, dimethylformamide; DTNB, 5'5'-dithio-bis(2-nitrobenzoic acid); DMEM, Dulbecco's modified Eagle medium; ^1H , hydrogen-1; K_D , dissociation constant; mAChR, muscarinic acetylcholine receptor; nAChR, nicotinic acetylcholine recep-

tor; PAS, peripheral anionic site; PLIP, protein ligand interaction profiler; R, resting state

REFERENCES

- (1) Karlin, A.; Akabas, M. H. Toward a structural basis for the function of nicotinic acetylcholine receptors and their cousins. *Neuron* **1995**, *15*, 1231–1244.
- (2) Changeux, J. P.; Edelstein, S. J. Allosteric receptors after 30 years. *Neuron* **1998**, *21*, 959–980.
- (3) Lindstrom, J. M. Nicotinic acetylcholine receptors of muscles and nerves: comparison of their structures, functional roles, and vulnerability to pathology. *Ann. N.Y. Acad. Sci.* **2003**, *998*, 41–52.
- (4) McKay, B. E.; Placzek, A. N.; Dani, J. A. Regulation of synaptic transmission and plasticity by neuronal nicotinic acetylcholine receptors. *Biochem. Pharmacol.* **2007**, *74*, 1120–1133.
- (5) Somm, E.; Guérardel, A.; Maouche, K.; Toulotte, A.; Veyrat-Durebex, C.; Rohner-Jeanrenaud, F.; Maskos, U.; Hüppi, P. S.; Schwitzgebel, V. M. Concomitant $\alpha 7$ and $\beta 2$ nicotinic AChR subunit deficiency leads to impaired energy homeostasis and increased physical activity in mice. *Mol. Genet. Metab.* **2014**, *112*, 64–72.
- (6) Dajas-Bailador, F.; Wonnacott, S. Nicotinic acetylcholine receptors and the regulation of neuronal signalling. *Trends Pharmacol. Sci.* **2004**, *25*, 317–324.
- (7) Albuquerque, E. X.; Pereira, E. F.; Alkondon, M.; Rogers, S. W. Mammalian nicotinic acetylcholine receptors: from structure to function. *Physiol. Rev.* **2009**, *89*, 73–120.
- (8) Gotti, C.; Clementi, F.; Fornari, A.; Gaimarri, A.; Guiducci, S.; Manfredi, I.; Moretti, M.; Pedrazzi, P.; Pucci, L.; Zoli, M. Structural and functional diversity of native brain neuronal nicotinic receptors. *Biochem. Pharmacol.* **2009**, *78*, 703–711.
- (9) Shen, J. X.; Yakel, J. L. Nicotinic acetylcholine receptor-mediated calcium signaling in the nervous system. *Acta Pharmacol. Sin.* **2009**, *30*, 673–680.
- (10) Clarke, P. B. The fall and rise of neuronal α -bungarotoxin binding proteins. *Trends Pharmacol. Sci.* **1992**, *13*, 407–413.
- (11) Sargent, P. B.; Garrett, E. N. The characterization of α -bungarotoxin receptors on the surface of parasympathetic neurons in the frog heart. *Brain Res.* **1995**, *680*, 99–107.
- (12) Nashmi, R.; Dickinson, M. E.; McKinney, S.; Jareb, M.; Labarca, C.; Fraser, S. E.; Lester, H. A. Assembly of $\alpha 4\beta 2$ Nicotinic Acetylcholine Receptors Assessed with Functional Fluorescently Labeled Subunits: Effects of Localization, Trafficking, and Nicotine-Induced Upregulation in Clonal Mammalian Cells and in Cultured Midbrain Neurons. *J. Neurosci.* **2003**, *23*, 11554–11567.
- (13) Scholze, P.; Ciurazskiewicz, A.; Groessl, F.; Orr-Urtreger, A.; McIntosh, J. M.; Huck, S. $\alpha 4\beta 2$ nicotinic acetylcholine receptors in the early postnatal mouse superior cervical ganglion. *Dev. Neurobiol.* **2011**, *71*, 390–399.
- (14) Ma, K. G.; Qian, Y. H. Alpha 7 nicotinic acetylcholine receptor and its effects on Alzheimer's disease. *Neuropeptides* **2019**, *73*, 96–106.
- (15) Hicks, D.; John, D.; Makova, N. Z.; Henderson, Z.; Nalivaeva, N. N.; Turner, A. J. Membrane targeting, shedding and protein interactions of brain acetylcholinesterase. *J. Neurochem.* **2011**, *116*, 742–746.
- (16) Massoulié, J.; Bon, S.; Perrier, N.; Falasca, C. The C-terminal peptides of acetylcholinesterase: cellular trafficking, oligomerization and functional anchoring. *Chem. Biol. Interact.* **2005**, *157–158*, 3–14.
- (17) Bartolini, M.; Bertucci, C.; Cavrini, V.; Andrisano, V. β -Amyloid aggregation induced by human acetylcholinesterase: inhibition studies. *Biochem. Pharmacol.* **2003**, *65*, 407–416.
- (18) Johnson, G.; Moore, S. W. The peripheral anionic site of acetylcholinesterase: structure, functions and potential role in rational drug design. *Curr. Pharm. Des.* **2006**, *12*, 217–225.
- (19) Nees, F. The nicotinic cholinergic system function in the human brain. *Neuropharmacol.* **2015**, *96*, 289–301.
- (20) Nasb, M.; Tao, W.; Chen, N. Alzheimer's Disease Puzzle: Delving into Pathogenesis Hypotheses. *Aging Dis.* **2024**, *15*, 43.

- (21) Binu, A.; Kumar, S. S.; Padma, U. D.; Madhu, K. Pathophysiological basis in the management of myasthenia gravis: a mini review. *Inflammopharmacol* **2022**, *30*, 61–71.
- (22) Terry, A. V., Jr.; Jones, K.; Bertrand, D. Nicotinic acetylcholine receptors in neurological and psychiatric diseases. *Pharmacol. Res.* **2023**, *191*, 106764.
- (23) Mazzaferro, S.; Msekela, D. J.; Cooper, E. C.; Maheshwari, A.; Sine, S. M. Genetic Variant in Nicotinic Receptor $\alpha 4$ -Subunit Causes Sleep-Related Hyperkinetic Epilepsy via Increased Channel Opening. *International J. Mol. Sci.* **2022**, *23*, 12124.
- (24) Steinlein, O. K.; Bertrand, D. Nicotinic receptor channelopathies and epilepsy. *Pflugers Arch* **2010**, *460*, 495–503.
- (25) Hernandez, C. M.; Dineley, K. T. $\alpha 7$ Nicotinic acetylcholine receptors in Alzheimer's disease: neuroprotective, neurotrophic or both? *Curr. Drug Targets* **2012**, *13*, 613–622.
- (26) Wang, H. Y.; Lee, D. H.; Davis, C. B.; Shank, R. P. Amyloid Peptide $A\beta_{1-42}$ Binds Selectively and with Picomolar Affinity to $\alpha 7$ Nicotinic Acetylcholine Receptors. *J. Neurochem.* **2000**, *75*, 1155–1161.
- (27) Burns, L. H.; Pei, Z.; Wang, H.-Y. Targeting $\alpha 7$ nicotinic acetylcholine receptors and their protein interactions in Alzheimer's disease drug development. *Drug Dev. Res.* **2023**, *84*, 1085–1095.
- (28) Servent, D.; Winckler-Dietrich, V.; Hu, H. Y.; Kessler, P.; Drevet, P.; Bertrand, D.; Ménez, A. Only Snake Curaremimetic Toxins with a Fifth Disulfide Bond Have High Affinity for the Neuronal $\alpha 7$ Nicotinic Receptor. *J. Biol. Chem.* **1997**, *272*, 24279–24286.
- (29) Lee, C. H.; Hung, S. Y. Physiologic Functions and Therapeutic Applications of $\alpha 7$ Nicotinic Acetylcholine Receptor in Brain Disorders. *Pharmaceutics* **2022**, *15*, 31.
- (30) Fabiani, C.; Murray, A. P.; Corradi, J.; Antollini, S. S. A novel pharmacological activity of caffeine in the cholinergic system. *Neuropharmacol* **2018**, *135*, 464–473.
- (31) Fabiani, C.; Biscussi, B.; Munafó, J. P.; Murray, A. P.; Corradi, J.; Antollini, S. S. New Synthetic Caffeine Analogs as Modulators of the Cholinergic System. *Mol. Pharmacol.* **2022**, *101*, 154–167.
- (32) Reshetnikov, D. V.; Ivanov, I. D.; Baev, D. S.; Rybalova, T. V.; Mozhaitev, E. S.; Patrushev, S. S.; Vavilin, V. A.; Tolstikova, T. G.; Shults, E. E. Design, Synthesis and Assay of Novel Methylxanthine–Alkynylmethylamine Derivatives as Acetylcholinesterase Inhibitors. *Molecules* **2022**, *27*, 8787.
- (33) Sharma, M.; Sharma, A.; Nuthakki, V. K.; Bhatt, S.; Nandi, U.; Bharate, S. B. Design, synthesis, and structure–activity relationship of caffeine-based triazoles as dual AChE and BACE-1 inhibitors. *Drug Dev. Res.* **2022**, *83*, 1803–1821.
- (34) Sharma, M.; Sharma, A.; Thakur, S.; Nuthakki, V. K.; Jamwal, A.; Nandi, U.; Jadhav, H. R.; Bharate, S. B. Discovery of blood-brain barrier permeable and orally bioavailable caffeine-based amide derivatives as acetylcholinesterase inhibitors. *Bioorg. Chem.* **2023**, *139*, 106719.
- (35) Elgazar, A. A.; El-Domany, R. A.; Eldehna, W. M.; Badria, F. A. Theophylline-based hybrids as acetylcholinesterase inhibitors endowed with anti-inflammatory activity: synthesis, bioevaluation, in silico and preliminary kinetic studies. *RSC Adv.* **2023**, *13* (36), 25616–25634.
- (36) Cheung, J.; Rudolph, M. J.; Burshteyn, F.; Cassidy, M. S.; Gary, E. N.; Love, J.; Franklin, M. C.; Height, J. J. Structures of human acetylcholinesterase in complex with pharmacologically important ligands. *J. Med. Chem.* **2012**, *55*, 10282–10286.
- (37) de Almeida, J. R.; Figueiro, M.; Almeida, W. P.; de Paula da Silva, C. H. T. Discovery of novel dual acetylcholinesterase inhibitors with antifibrillogenic activity related to Alzheimer's disease. *Fut Med. Chem.* **2018**, *10*, 1037–1053.
- (38) Shafferman, A.; Velan, B.; Ordentlich, A.; Kronman, C.; Grosfeld, H.; Leitner, M.; Flashner, Y.; Cohen, S.; Barak, D.; Ariel, N. Substrate inhibition of acetylcholinesterase: residues affecting signal transduction from the surface to the catalytic center. *EMBO J.* **1992**, *11*, 3561–3568.
- (39) Dvir, H.; Silman, I.; Harel, M.; Rosenberry, T. L.; Sussman, J. L. Acetylcholinesterase: from 3D structure to function. *Chem. Biol. Interact* **2010**, *187*, 10–22.
- (40) Pohanka, M. Cholinesterases, a target of pharmacology and toxicology. *Biomed. Pap. Med. Fac. Palacky Univ. Olomouc Czech Repub.* **2011**, *155*, 219–223.
- (41) Colovic, M. B.; Krstic, D. Z.; Lazarevic-Pasti, T. D.; Bondzic, A. M.; Vasic, V. M. Acetylcholinesterase inhibitors: pharmacology and toxicology. *Curr. Neuropharmacol.* **2013**, *11*, 315–335.
- (42) Sakmann, B.; Patlak, J.; Neher, E. Single acetylcholine-activated channels show burst-kinetics in presence of desensitizing concentrations of agonist. *Nature* **1980**, *286*, 71–73.
- (43) Bouzat, C.; Barrantes, F.; Sine, S. Nicotinic receptor fourth transmembrane domain: hydrogen bonding by conserved threonine contributes to channel gating kinetics. *J. Gen. Physiol.* **2000**, *115*, 663–672.
- (44) Bouzat, C.; Gumilar, F.; del Carmen Esandi, M.; Sine, S. M. Subunit-selective contribution to channel gating of the M4 domain of the nicotinic receptor. *Biophys. J.* **2002**, *82*, 1920–1929.
- (45) Corradi, J.; Spitzmaul, G.; De Rosa, M. J.; Costabel, M.; Bouzat, C. Role of pairwise interactions between M1 and M2 domains of the nicotinic receptor in channel gating. *Biophys. J.* **2007**, *92*, 76–86.
- (46) Lurtz, M. M.; Pedersen, S. E. Aminotriarylmethane dyes are high-affinity noncompetitive antagonists of the nicotinic acetylcholine receptor. *Mol. Pharmacol.* **1999**, *55*, 159–167.
- (47) Zarkadas, E.; Pebay-Peyroula, E.; Thompson, M. J.; Schoehn, G.; Uchanski, T.; Steyaert, J.; Chipot, C.; Dehez, F.; Baenziger, J. E.; Nury, H. Conformational transitions and ligand-binding to a muscle-type nicotinic acetylcholine receptor. *Neuron* **2022**, *110*, 1358–1370.e5.
- (48) Hansen, S. B.; Sulzenbacher, G.; Huxford, T.; Marchot, P.; Taylor, P.; Bourne, Y. Structures of Aplysia AChBP complexes with nicotinic agonists and antagonists reveal distinctive binding interfaces and conformations. *EMBO J.* **2005**, *24*, 3635–3646.
- (49) Hibbs, R. E.; Sulzenbacher, G.; Shi, J.; Talley, T. T.; Conrod, S.; Kem, W. R.; Taylor, P.; Marchot, P.; Bourne, Y. Structural determinants for interaction of partial agonists with acetylcholine binding protein and neuronal $\alpha 7$ nicotinic acetylcholine receptor. *EMBO J.* **2009**, *28* (19), 3040–3051.
- (50) Spurny, R.; Debaveye, S.; Farinha, A.; Veys, K.; Vos, A. M.; Gossas, T.; Attack, J.; Bertrand, S.; Bertrand, D.; Danielson, U. H.; Tresadern, G.; Ulens, C. Molecular blueprint of allosteric binding sites in a homologue of the agonist-binding domain of the $\alpha 7$ nicotinic acetylcholine receptor. *Proc. Natl. Acad. Sci. U.S.A.* **2015**, *112*, 2543–2552.
- (51) Grutter, T.; Prado de Carvalho, L.; Le Novère, N.; Corringer, P. J.; Edelstein, S.; Changeux, J.-P. An H-bond between two residues from different loops of the acetylcholine binding site contributes to the activation mechanism of nicotinic receptors. *EMBO J.* **2003**, *22*, 1990–2003.
- (52) Xiu, X.; Puskar, N. L.; Shanata, J. A. P.; Lester, H. A.; Dougherty, D. A. Nicotine binding to brain receptors requires a strong cation-pi interaction. *Nature* **2009**, *458*, 534–537.
- (53) Karlin, A. Emerging structure of the nicotinic acetylcholine receptors. *Nat. Rev. Neurosci.* **2002**, *3*, 102–114.
- (54) Blum, A. P.; Lester, H. A.; Dougherty, D. A. Nicotinic pharmacophore: the pyridine N of nicotine and carbonyl of acetylcholine hydrogen bond across a subunit interface to a backbone NH. *Proc. Natl. Acad. Sci. U.S.A.* **2010**, *107*, 13206–13211.
- (55) Bruhova, I.; Auerbach, A. Molecular recognition at cholinergic synapses: acetylcholine versus choline. *J. Physiol.* **2017**, *595*, 1253–1261.
- (56) Medina-Moreno, A.; Henriquez, J. P. Maturation of a postsynaptic domain: Role of small Rho GTPases in organising nicotinic acetylcholine receptor aggregates at the vertebrate neuromuscular junction. *J. Anat.* **2022**, *241*, 1148–1156.
- (57) Barrantes, F. J. Oligomeric forms of the membrane-bound acetylcholine receptor disclosed upon extraction of the Mr 43,000 nonreceptor peptide. *J. Cell Biol.* **1982**, *92*, 60–68.
- (58) Ellman, G. L.; Courtney, K. D., Jr.; Andres, V.; Featherstone, R. M. A new and rapid colorimetric determination of acetylcholinesterase activity. *Biochem. Pharmacol.* **1961**, *7*, 88–95.

- (59) Chrestia, J. F.; Oliveira, A. S.; Mulholland, A. J.; Gallagher, T.; Bermúdez, I.; Bouzat, C. A Functional Interaction Between Y674-R685 Region of the SARS-CoV-2 Spike Protein and the Human $\alpha 7$ Nicotinic Receptor. *Mol. Neurobiol.* **2022**, *59*, 6076–6090.
- (60) Nieves, G. A. F.; Barrantes, F. J.; Antollini, S. S. Modulation of nicotinic acetylcholine receptor conformational state by free fatty acids and steroids. *J. Biol. Chem.* **2008**, *283*, 21478–21486.
- (61) Pettersen, E. F.; Goddard, T. D.; Huang, C. C.; Couch, G. S.; Greenblatt, D. M.; Meng, E. C.; Ferrin, T. E. UCSF Chimera: a visualization system for exploratory research and analysis. *J. Comput. Chem.* **2004**, *25*, 1605–1612.
- (62) Trott, O.; Olson, A. J. AutoDock Vina: improving the speed and accuracy of docking with a new scoring function, efficient optimization and multithreading. *J. Comput. Chem.* **2010**, *31*, 455–461.
- (63) Eberhardt, J.; Santos-Martins, D.; Tillack, A. F.; Forli, S. AutoDock Vina 1.2.0: New Docking Methods, Expanded Force Field, and Python Bindings. *J. Chem. Inf. Mod.* **2021**, *61*, 3891–3898.
- (64) Wallace, A. C.; Laskowski, R. A.; Thornton, J. M. LIGPLOT: a program to generate schematic diagrams of protein-ligand interactions. *Protein Eng.* **1995**, *8*, 127–134.
- (65) Laskowski, R. A.; Swindells, M. B. LigPlot+: multiple ligand-protein interaction diagrams for drug discovery. *J. Chem. Inf. Model.* **2011**, *51*, 2778–2786.
- (66) Adasme, M. F.; Linnemann, K. L.; Bolz, S. N.; Kaiser, F.; Salentin, S.; Haupt, V. J.; Schroeder, M. PLIP 2021: expanding the scope of the protein–ligand interaction profiler to DNA and RNA. *Nucleic Acids Res.* **2021**, *49*, W530–W534.